



The prediction method for standard enthalpies of apatites using the molar volume, lattice energy, and linear correlations from existing experimental data

Bartosz Puzio¹ · Maciej Manecki¹

Received: 21 April 2022 / Accepted: 27 September 2022 / Published online: 25 October 2022
© The Author(s) 2022

Abstract

Experimental data of thermodynamic state functions and molar volume for phosphate, arsenate, and vanadate apatites containing Ca, Sr, Ba, Pb, and Cd at the cationic positions Me^{2+} and F, OH, Cl, Br, and I at the halide position X were collected. The apatite supergroup splits into distinct subgroups (populations) constituted by $\text{Me}_{10}(\text{AO}_4)_6\text{X}_2$ with the same Me^{2+} cations and tetrahedral AO_4^{3-} anions but with different anions at the X position. Linear relationships between various parameters within apatite subgroups are observed. The prediction method for standard enthalpies of apatites ($\Delta H^\circ_{\text{f},\text{el}}$) is based on regression analysis of the linear correlations within the subgroups between $\Delta H^\circ_{\text{f},\text{el}}$ of apatites and their molar volume V_m , lattice energy U_{POT} , and $\Delta H^\circ_{\text{f},\text{el}}$ of their anions AO_4^{3-} or X^- . This allowed to predict 22 new $\Delta H^\circ_{\text{f},\text{el}}$ values for apatites and materials with an apatite structure. The prediction precision is comparable to the experimental uncertainty obtained when reproducing experimental data using calorimetric measurements or dissolution experiments and can be applied to a wider range of apatites than other methods.

Keywords Iodoapatites · Thermodynamics of apatites · Thermodynamic stability · Volume-based Thermodynamics · Thermodynamic database

Introduction

Quantitative geochemical calculations are not possible without thermodynamic databases. Considerable advances in the quantity and quality of these databases have been made since the early days of Lewis and Randall (1923), Latimer (1952), and Rossini et al. (1952). According to Oelkers and Shott (2018), the emergence of thermodynamic databases can be considered one of the greatest advances in geochemistry of the last century. Thermodynamic data have been used in basic research and for countless applications in computational modelling, computer simulations, waste management, and policy-making. The challenges today are to evaluate thermodynamic data for internal consistency

and to reach a most reliable properties. The present work focuses on the enthalpy of formation from elements ($\Delta H^\circ_{\text{f},\text{el}}$) of minerals and synthetic compounds belonging to the apatite supergroup.

The natural apatites and apatite-based materials are a class of compounds with the stoichiometry $\text{Me}_{10}(\text{AO}_4)_6\text{X}_2$, where the Me-site is occupied by larger monovalent (Na^+ , K^+ , etc.), divalent (Ca^{2+} , Sr^{2+} , Ba^{2+} , Pb^{2+} , Cd^{2+} , etc.), or trivalent (La^{3+} , Y^{3+} , Ce^{3+} , Sm^{3+} , etc.) cations, the A-site is occupied by a smaller metal, metalloid or nonmetal (P^{5+} , As^{5+} , V^{5+} , Si^{4+} , etc., often accompanied by carbonate anion CO_3^{2-}), and the X-site is filled by halides, hydroxides, or oxides (F^- , Cl^- , Br^- , I^- , OH^- , O^{2-} , etc., also often accompanied by a carbonate anion CO_3^{2-}) (e.g., Rakovan and Hughes 2000; Pan and Fleet 2002; Pasero et al. 2010; Tait et al. 2015; Ptáček 2016; Hughes and Rakovan 2018; Pieczka 2018; Rakovan and Scovil 2021). Due to the extremely rich array of possible substitutions in each of the highlighted positions, the possible end-members alone are over 200 types, indicating that this is currently the most numerous supergroup of minerals and compounds (Baker 1966; Oelkers and Valsami-Jones 2008; Rakovan

Communicated by Mark S Ghiorso.

✉ Bartosz Puzio
bpuzio@agh.edu.pl

¹ Department of Mineralogy, Petrography and Geochemistry, AGH University of Science and Technology, al. Mickiewicza 30, 30-059 Kraków, Poland

and Pasteris 2015; Flora et al. 2004a, b). Synthesis methods are also still being developed to produce apatite-based materials, which have enormous applications in numerous technologies (Oelkers and Montel 2008; Cao et al. 2017; Lei et al. 2020). Unfortunately, for many of the apatites, there is a lack of experimentally determined basic thermodynamic data including $\Delta H^\circ_{\text{f},\text{el}}$. This includes some representatives of the best-characterized phosphate apatites (e.g., $\text{Ba}_{10}(\text{PO}_4)_6\text{Br}_2$, $\text{Sr}_{10}(\text{PO}_4)_6\text{Br}_2$ or $\text{Cd}_{10}(\text{PO}_4)_6\text{Br}_2$) as well as most arsenate and vanadate apatites. As of the current state of knowledge, there is not a single experimentally measured $\Delta H^\circ_{\text{f},\text{el}}$ for iodine-containing apatite-based materials, which are the subject of intense research due to potential technological uses (Wang 2015; Hartnett et al. 2019; Merker and Wondratschek 1959; Brenner et al. 1970; Sudarsanan et al. 1977; Audubert et al. 1999; Alberius et al. 1999; Stennett et al. 2011; Lu et al. 2014; Suetsugu 2014; Witkowska et al. 2014; Coulon et al. 2017; Mungmode et al. 2018; Sordyl et al. 2020; Islam 2021). However, with relatively little effort, gaps in thermodynamic databases can be filled using predictive methods.

Several attempts have been made to fill the gaps in the thermodynamic databases using predictive methods e.g., Volume-based Thermodynamics (VBT; Jenkins and Glasser 2003; Glasser and Jenkins 2016), the Simple Salt Approximation (SSA; Yoder and Flora 2005; Yoder and Rowand 2006; Glasser 2019), and the polyhedral contribution approach (Latimer 1951, 1952; Hazen 1985; Chermak and Rimistidt 1989; La Iglesia and Felix 1994; Glasser and Jenkins 2009; La Iglesia 2009; Drouet 2015, 2019). Moreover, the predictions based on linear correlations between thermodynamic state functions and selected physicochemical parameters gives promising results (Tardy and Vieillard 1977; Vieillard and Tardy 1988; Sassani and Shock 1992; Shock et al. 1997; Sverjensky et al. 1997; Vieillard 2000; Cruz et al. 2005a, b; Puzio et al. 2022). The ThermAP method by Drouet (2015 and 2019) gives the best accuracy approaching $\pm 1\%$ absolute error. However, in the case of apatites, an uncertainty of $\pm 1\%$ is too high: $\Delta H^\circ_{\text{f},\text{el}}$ determined experimentally for $\text{Ca}_{10}(\text{PO}_4)_6\text{Cl}_2$ and $\text{Ca}_{10}(\text{PO}_4)_6\text{Br}_2$ differ only by 0.8% (58 kJ mol⁻¹; Cruz et al. 2005b).

In the present study the experimental data of thermodynamic state functions and molar volume for phosphate, arsenate, and vanadate apatites containing Ca, Sr, Ba, Pb, and Cd at the cationic positions Me^{2+} and F, OH, Cl, Br, and I at the halide position X were collected. Linear relationships between various parameters within apatite subgroups are examined. A new prediction method for standard enthalpies of apatites is proposed. This approach is based on regression analysis of the linear correlations within the subgroups between $\Delta H^\circ_{\text{f},\text{el}}$ of apatites and their molar volume V_m , lattice energy U_{POT} , and $\Delta H^\circ_{\text{f},\text{el}}$ of their anions AO_4^{3-} or X^- .

Overview of experimental thermodynamic data of apatites

Table 1 provides a compilation of the thermodynamic data available in the literature (based on experiments and "ab initio" calculations) for stoichiometric $\text{Me}_{10}(\text{AO}_4)_6X_2$ apatites (phosphate, arsenate, and vanadate with different Me^{2+} and X^-), such as the standard enthalpy of formation from elements $\Delta H^\circ_{\text{f},\text{el}}$, the standard entropy $S^\circ_{298.15\text{K}}$, the specific heat capacity $C^\circ_{\text{p,m}}$, the molar volume V_m , and the solubility constant $K_{\text{sp},298.15\text{K}}$. The Gibbs free energy of formation ($\Delta G^\circ_{\text{f},\text{el}}$) is not included to maintain consistency in the thermodynamic data presented. $\Delta G^\circ_{\text{f},\text{el}}$ values available in the literature are mostly calculated from approximations or using different, often mixed thermodynamic databases, which contributes significant scatter. Therefore, the compilation and variability analysis of the $\Delta G^\circ_{\text{f},\text{el}}$ data for apatites should be discussed in a separate paper.

The observed discrepancies in the data are likely due to the varying crystallinity states, polymorphs (either hexagonal or monoclinic, mostly not identified in literature reports), nonstoichiometry, hydration state and/or the presence of undetected impurities. A lower degree of crystallinity, for example, may favor somewhat less negative values of $\Delta H^\circ_{\text{f},\text{el}}$ (Craig and Rootare 1974). The difference between the hexagonal ($P6_3/m$) and monoclinic ($P2_1/b$) symmetries results in different positioning of the X^- anions along the apatitic channels (giving rise or not to a mirror plane) but does not correspond to a large ion rearrangement. Therefore, the energetics of formation are not expected to be very different (although not identical), allowing both polymorphs to be considered equal.

Drouet (2015) and Puzio et al. (2022) previously reported that thermodynamic state functions for apatites vary in a regular, mostly linear manner, depending on various physicochemical parameters of their components, such as the ionic radius of X^- , the electronegativity of X^- , the ionization energy of X, and others. A current and complete review of the data presented in Table 1 allows such trends and relationships to be clearly observed. For example, for a given X^- anion (from among OH^- , F^- , Cl^- , or Br^-), the formation of apatite is less exothermic (the enthalpy of formation $\Delta H^\circ_{\text{f},\text{el}}$ is less negative) when apatite contains a heavier element, such as As or V instead of P and Cd or Pb instead of alkali metals (Fig. 1A). In contrast, this relationship is not observed when alkali metals (Ca^{2+} , Ba^{2+} or Sr^{2+}) are substituted in the Me^{2+} position. It is clearly apparent from the graph that apatites form distinctly separate subgroups (Fig. 1A). Here, a subgroup is defined as a population of apatites with the same substitution at position Me and A but with different substitutions at position X (where X = F, Cl, Br, I, OH) e.g., subgroup of

Table 1 Experimental-based and “ab initio” literature data available for apatite end-members with the general chemical formula $\text{Me}_{10}(\text{AO}_4)_6\text{X}_2$ (where $\text{Me} = \text{Ca}, \text{Ba}, \text{Sr}, \text{Pb}, \text{Cd}; \text{A} = \text{P}, \text{As}, \text{V}$, and $\text{X} = \text{F}, \text{OH}, \text{Cl}, \text{Br}, \text{I}$, at $T = 298 \text{ K}$ and 1 bar)

Chemical formula	$\Delta H_{\text{ref}}^{\circ}$ (kJ mol $^{-1}$)	Reference	S° (J mol $^{-1}$ K $^{-1}$)	Reference	$C^{\circ}_{p, m}$ (J mol $^{-1}$ K $^{-1}$)	Reference	$\log K_{\text{sp}}$	Reference	V_{m} (nm 3)	Reference
$\text{Ca}_{10}(\text{PO}_4)_6\text{F}_2$	-13,449	Yan et al. 2020	766.4	Dachs et al. 2010	739.2	Dachs et al. 2010	-118.0	Stumm and Morgan 2012	0.5236	Lim et al. 2011
-13,548	Cherifa and Jemal 2004	765.0	Flora et al. 2004a, b	646.0	Cruz et al. 2005a, b	-111.4	Zhu et al. 2009	0.5237	O'Donnell et al. 2009	
-13,558	Flora et al. 2004a, b	771.8	Bogach et al. 2001	740.9	Fleche 2002	-58.8	Harouya et al. 2007	0.5246	Mercier et al. 2007	
-13,550	Ntahomvukiye et al. 1997	775.8	Robie and Hem- ingway 1995	751.0	Bogach et al. 2001	-61.9	Stefansson 2001	0.5231	ICDD 1997	
-13,545	Jemal et al. 1995	775.7	Wagman et al. 1982	751.8	Robie and Hem- ingway 1995	-116.3	Jaynes et al. 1999	0.5233	Sudarsanan et al. 1972	
-13,744	Robie and Hem- ingway 1995	776.5	Egan et al. 1951	751.6	Roine 1994	-65.9	Valsami-Jones et al. 1998			
-13,536	Cherifa et al. 1991			756.2	Zhu and Sver- jenksy 1991	-50.9	Elliot 1994			
-13,653	Zhu and Sver- jenksy 1991			752.0	Vieillard and Tardy 1984	-120.1	Chin and Nan- collas 1991			
-13,657	Valyashko et al. 1968			751.9	Wagman et al. 1982	-119.2	LeGeros 1991			
-13,677	Farr and Elmore 1962			751.0	Mooney and Aia 1961	-121.2	Driessens 1982			
-13,684	Smirnova et al. 1962			752.3	Egan et al. 1951	-120.3	Anjaj et al. 1981			
-13,797	Jacques 1963				-3.8		Ball et al. 1980			
-13,719	Kelley and King 1961				-120.7		Farr and Elmore 1962			
-13,655	Gotschall 1958				-117.8		Lindsay 1979			
					-140.8		Robie et al. 1979			
					-120.3		McCann 1968			
					-119.2		McCann 1968			
					-7.1		Valyashko et al. 1968			
					-2.2		Lindsay and Moreno 1960			
$\text{Ca}_{10}(\text{PO}_4)_6\text{OH}_2$	-13,710	Puzio et al. 2018	768.0	Flora et al. 2004a, b	694.0	Cruz et al. 2005a, b	-115.8	Puzio et al. 2018	0.5300	Puzio et al. 2018
-13,431	Rollin-Martinet et al. 2013	785.0	Bogach et al. 2001	765.8	Bogach et al. 2001	-116.8	Zhu et al. 2016	0.5243	Chernorukov et al. 2011	

Table 1 (continued)

Chemical formula	$\Delta H_{\text{rel}}^{\circ}$ (kJ mol ⁻¹)	Reference	S° (J mol ⁻¹ K ⁻¹)	Référence	$C^{\circ}_{p, m}$ (J mol ⁻¹ K ⁻¹)	Référence	$\log K_{\text{sp}}$	Référence	V_m (nm ³)	Reference	
-13,399	Cruz et al. 2005a,b	780.8	Robie and Hemingway 1995	770.1	Robie and Hemingway 1995	-106.6	Zhang et al. 2011	0.5298	Lee et al. 2009		
-13,314	Flora et al. 2004a,b	797.9	Zhu and Sverjensky 1991	769.9	Wagman et al. 1982	-106.6	Zhu et al. 2009	0.5252	Cruz et al. 2005a,b		
-13,508	Krivitsov et al. 1997	780.7	Wagman et al. 1982	772.6	Mooney and Aia 1961	-52.0	Stefansson 2001	0.5309	Kim et al. 2000		
-13,305	Jemal et al. 1995	781.1	Egan et al. 1951	770.2	Kelley et al. 1960	-112.0	Jaynes et al. 1999	0.5288	ICDD 1997		
-13,443	Roine 1994			770.2	Egan et. al. 1951	-114.0	Stumm and Morgan 2012	0.5289	Elastri et al. 1995		
-13,292	Cherifa et al. 1991			801.1	Egan et. al. 1950	-123.0	Ito et al. 1996	0.5270	Phebe and Narasraju 1995		
-13,396	Zhu and Sverjensky 1991					-115.5	Shellis et al. 1993	0.5296	Ben Cherifa et al. 1988		
-13,477	Vieillard and Tardy 1984					-115.3	LeGeros 1991	0.5287	McConell 1974		
-13,422	Valyashko et al. 1968					-112.1	Moreno and Aoja 1991	0.5291	Sudarsanan and Young 1969		
-13,517	Jacques 1963					-119.8	Gramain et al. 1987	0.5301	Posner et al. 1958		
-13,445	Smirnova et al. 1962					-110.6	Narasraju et al. 1979				
-13,525	Gottschall 1958					-115.1	Bell et al. 1978				
						-116.6	McDowell et al. 1977				
						-118.0	Santillan-Medrano 1975				
						-116.4	Avnimelech et al. 1973				
						-109.2	Moreno et al. 1968				
<chem>Ca10(PO4)6Cl2</chem>	-13,231	Cruz et al. 2005a,b	808.0	Babu et al. 2011	747.8	Dachs et al. 2010	-112.3	Narasraju et al. 1979	0.5371	Cruz et al. 2005a,b	
-13,119	Cherifa and Jemal 2004	801.2	Dachs et al. 2010	608.0	Gotherstrom et al. 2002			0.5419	El Feki et al. 2004		
-13,179	Jemal 2004	804.3	Bogach et al. 2001	756.0	Tacker and Stormer 1989			0.5421	ICDD 2004		
-13,180	Flora et al. 2004a,b	800.2	Zhu and Sverjensky 1991	762.0	Zhu and Sverjensky 1991			0.5561	White and Dong 2003		

Table 1 (continued)

Chemical formula	$\Delta H_{\text{rel}}^{\circ}$ (kJ mol ⁻¹)	Reference	S° (J mol ⁻¹ K ⁻¹)	Référence	$C_{p,m}^{\circ}$ (J mol ⁻¹ K ⁻¹)	Référence	$\log K_{\text{sp}}$	Référence	V_m (nm ³)	Référence
	-13,139	Khattech and Jemal 1997	795.8	Vieillard and Tardy 1984	758.0	Krishnan et al. 2008			0.5389	Kim et al. 2000
	-13,161	Cherifa et al. 1991	796.2	Valyashko et al. 1968	751.0	Babu et al. 2011			0.5450	ICDD 1997
-13,201	Zhu and Sverjensky 1991				752.6	Bogach et al. 2001			0.5448	Ben Cherifa et al. 1991
	-13,096	Tacker and Storner 1989			758.3	Valyashko et al. 1968			0.5450	Mayer et al. 1979
	-13,278	Gottschall 1958							0.5445	Sudarsanan and Young 1978
									0.5430	Mackie et al. 1972
									0.5455	Bhatnagar 1970
									0.5486	Cruz et al. 2005a , ^b
									0.5561	White and Dong 2003
									0.5561	Elliot et al. 1981
									0.5560	Dykes 1974
									0.5440	Phebe and Narasaraju 1995
									Not shown	Coulon et al. 2016
									0.5484	Alberius Henning et al. 1999
									0.6178	Jain et al. 2013
									0.5695	Yuan et al. 2017
									0.6010	Knyazev et al. 2015
									0.6010	Chernorukov et al. 2011
									0.5961	Lim et al. 2011
									0.5964	Aissa et al. 2004
									0.5958	ICDD 2004
									0.5901	Swafford and Holt 2002
									0.5967	ICDD 1997
									0.5952	Corker et al. 1995
									0.5944	McConell 1974

Table 1 (continued)

Chemical formula	$\Delta H_{\text{rel}}^{\circ}$ (kJ mol ⁻¹)	Reference	S° (J mol ⁻¹ K ⁻¹)	Référence	$C^{\circ}_{p, m}$ (J mol ⁻¹ K ⁻¹)	Référence	$\log K_{\text{sp}}$	Référence	V_m (nm ³)	Référence
$\text{Sr}_{10}(\text{PO}_4)_6\text{OH}_2$	-13,373	Jemal et al. 1995 –	–	–	–	–	–	–	0.5955	ICDD 2004
									0.5971	Mayer et al. 1979
									0.6010	Verbeeck et al. 1977
									0.6006	McConnell 1974
									0.5975	Sudarsanan and Young 1974
									0.5948	Klement 1939
									0.6305	Jain et al. 2013
									0.5786	Yuan et al. 2017
									0.6015	Knyazev et al. 2015
									0.6015	Chernorukov et al. 2011
									0.6152	ICDD 2004
									0.6152	ICDD 1997
									0.6073	Notzold et al. 1994
									0.6066	McConnell 1974
									0.6066	Sudarsanan and Young 1974
									0.6434	Jain et al. 2013
									0.5902	Yuan et al. 2017
									0.5991	Knyazev et al. 2015
									0.6213	Alberius–Henning et al. 2000
									0.6959	Junhui et al. 2016
									0.6947	Junhui et al. 2016
									0.6922	Junhui et al. 2016
									0.6890	Junhui et al. 2016
									0.6914	Aissa et al. 2004
									0.6904	ICDD 2004
									0.6951	ICDD 1997

Table 1 (continued)

Chemical formula	$\Delta H_{\text{rel}}^{\circ}$ (kJ mol ⁻¹)	Reference	S° (J mol ⁻¹ K ⁻¹)	Reference	$C^{\circ}_{p, m}$ (J mol ⁻¹ K ⁻¹)	Reference	$\log K_{\text{sp}}$	Reference	V_m (nm ³)	Reference
$\text{Ba}_{10}(\text{PO}_4)_6\text{OH}_2$	-13,309	Ben Cherifa and Jemal 2004	—	—	—	—	—	—	0.6903	Mathew et al. 1979
$\text{Ba}_{10}(\text{PO}_4)_6\text{Cl}_2$	-13,348	Junhui et al. 2016	1044.0	Babu et al. 2011	767.0	Babu et al. 2011	—	—	0.6874	McConnell 1974
$\text{Ba}_{10}(\text{PO}_4)_6\text{Br}_2$	-13,246	Khattech et al. 1996	—	—	787.0	Jena et al. 2011	—	—	0.6943	Lim et al. 2011
									0.6893	Duan et al. 2005
									0.6944	ICDD 2004
									Not shown	Bondareva and Malinovskii 1986
									0.6968	Bigi et al. 1984
									0.6924	McConnell 1974
									0.6924	Klement 1936
									0.7056	Junhui et al. 2016
									0.7036	Junhui et al. 2016
									0.6995	Junhui et al. 2016
									0.6954	Chernorukov et al. 2011
									0.7008	ICDD 2004
									0.6965	ICDD 1997
									0.6951	Newberry et al. 1981
									0.7008	Hata et al. 1979
									0.6974	McConnell 1974
									0.7159	Junhui et al. 2016
									0.7146	Junhui et al. 2016
									0.7126	Junhui et al. 2016
									0.7097	Junhui et al. 2016
									0.7107	Alberius-Henning et al. 2000

Table 1 (continued)

Table 1 (continued)

Chemical formula	$\Delta H_{\text{rel}}^{\circ}$ (kJ mol ⁻¹)	Reference	S° (J mol ⁻¹ K ⁻¹)	Référence	$C^{\circ}_{p, m}$ (J mol ⁻¹ K ⁻¹)	Référence	$\log K_{\text{sp}}$	Référence	V_m (nm ³)	Référence
Pb ₁₀ (PO ₄) ₆ OH ₂	-8261 -8220	Jemal et al. 1995 Zhu et al. 2015a	-	-	-	-	-161.5 -125.6	Zhu et al. 2016 Allison et al. 1991	0.6062 0.6260	Olds et al. 2021 ICDD 2004
										Kim et al. 1997
										Mayer et al. 1979
										McConnell 1974
										Davis 1973
										Engel 1970
										Gu et al. 2020
Pb ₁₀ (PO ₄) ₆ Cl ₂	-8216	Puzio et al. 2021	1244.0	Topolska et al. 2016	804.0	Topolska et al. 2016	-159.1	Puzio et al. 2021	0.6348	
	-8217	Topolska et al. 2016	1170.6	Bisengalieva et al. 2010	826.0	Bisengalieva et al. 2010	-159.2	Topolska et al. 2016	0.6297	Antao and Dhali- wal 2018
	-8248	Bisengalieva et al. 2010					-159.0	Drouet et al. 2015	0.6350	Antao and Dhali- wal 2018
	-7474	Chernorukov et al. 2010					-159.3	Flis et al. 2011	0.6321	Solecka et al. 2018
	-8220	Flora et al. 2004a, b					-161.7	Manecki and Maurice 2008	0.6336	Okudera 2013
	-8204	Jemal et al. 2004					-160.8	Xie and Giam- mar 2007	0.6323	Chernorukov et al. 2011
							-167.5	Manecki et al. 2000	0.6316	Chernorukov et al. 2010
							-168.8	Allison et al. 1992	0.6349	Flis et al. 2010
							-168.0	Nriagu 1973	0.6268	ICDD 2004
									0.6315	Kim et al. 2000
									0.6332	ICDD 1997
									0.6336	Dai and Hughes 1989
									0.6344	McConnell 1974
									0.6301	Merker and Won- dratschek 1957
Pb ₁₀ (PO ₄) ₆ Br ₂	-8180	Flora et al. 2004a, b	-	-	-	-	-154.8 -156.2	Janicka et al. 2012 Nriagu 1973	0.6480 0.6548	Janicka et al. 2012 ICDD 1997 ICDD 1997

Table 1 (continued)

Chemical formula	$\Delta H_{\text{rel}}^{\circ}$ (kJ mol ⁻¹)	Reference	S° (J mol ⁻¹ K ⁻¹)	Reference	$C_{\text{p}, \text{m}}^{\circ}$ (J mol ⁻¹ K ⁻¹)	Reference	$\log K_{\text{sp}}$	Reference	V_{m} (nm ³)	Reference
$\text{Pb}_{10}(\text{PO}_4)_6\text{I}_2$	-8042	Puzio et al. 2022	-	-	-	-	-	-	-	Merker and Wondratschek 1957
$\text{Pb}_{9,14}(\text{PO}_4)_6\text{I}_{0,26}$	-	-	-	-	-	-	-	-	0.6281	Bulanov et al. 2021
$\text{Ca}_{10}(\text{AsO}_4)_6\text{F}_2$	-11,259	Zhu et al. 2011	-	-	-78.42	Li et al. 2012	-	Noel 2018	-	
	-11,279	Li et al. 2012	-	-	-78.42	Zhu et al. 2011	-	Not shown	Karbovsky and Soroka 2014	
								0.5721	Biagioni and Pasero 2013	
$\text{Ca}_{10}(\text{AsO}_4)_6\text{OH}_2$	-11,208	Puzio et al. 2018	937.7	Zheng et al. 2015	-	-78.4	Puzio et al. 2018	0.5652	Baikie et al. 2007	
	-10,935	Puzio et al. 2018	-	-	-81.7	Zhu et al. 2012	-	0.5265	Puzio et al. 2018	
					-78.4	Zhu et al. 2006	0.5704	Not shown	Karbovsky and Soroka 2014	
	-11,156	Mahapatra et al.	1987	-	-83.2	Zhu et al. 2006	0.5708	Henderson et al. 2009	0.5704	Biagioni and Pasero 2013
				-	-80.2	Zhu et al. 2006	0.5711	Lee et al. 2009	0.5711	
				-	-76.1	Bothe and Brown 1999	0.6705	Mahapatra et al. 1989	0.6705	
				-	-89.8	Mahapatra et al. 1987	-	Dunn et al. 1980	0.5647	
				-	-94.5	Narasaraju et al. 1979	-	Mayer et al. 1979	0.5681	
				-	-	-	0.5852	Biagioni et al. 2017	-	
$\text{Ca}_{10}(\text{AsO}_4)_6\text{Cl}_2$	-	-	-	-	-	-	-	Not shown	Karbovsky and Soroka 2014	
								0.5984	Wardojo and Hwu 1996	
$\text{Ca}_{10}(\text{AsO}_4)_6\text{Br}_2$	-	-	-	-	-	-	-	0.6460	Wardojo and Hwu 1996	
								0.5724	Dunn et al. 1985	
								Not shown	Karbovsky and Soroka 2014	

Table 1 (continued)

Chemical formula	$\Delta H^\circ_{\text{rel}}$ (kJ mol ⁻¹)	Reference	S° (J mol ⁻¹ K ⁻¹)	Reference	$C^\circ_{p, m}$ (J mol ⁻¹ K ⁻¹)	Reference	$\log K_{\text{sp}}$	Reference	V_m (nm ³)	Reference
$\text{Sr}_{10}(\text{AsO}_4)_6\text{F}_2$	–	–	–	–	–	–	–	–	–	0.6392 Dordevic et al. 2008
$\text{Sr}_{10}(\text{AsO}_4)_6\text{OH}_2$	–	–	–	–	–	–	–	–	–	0.6396 Kreidler and Hummel 1970
$\text{Sr}_{10}(\text{AsO}_4)_6\text{Cl}_2$	–	–	–	–	–	–	–	–	–	0.6466 Weil et al. 2009
$\text{Sr}_{10}(\text{AsO}_4)_6\text{Br}_2$	–	–	–	–	–	–	–	–	–	0.6439 Mayer et al. 1979
$\text{Ba}_{10}(\text{AsO}_4)_6\text{F}_2$	–	–	–	–	–	–	–	–	–	0.6556 Bell et al. 2009
$\text{Ba}_{10}(\text{AsO}_4)_6\text{OH}_2$	–	–	–	–	–	–	–	–	–	0.6554 Weil et al. 2009
$\text{Ba}_{10}(\text{AsO}_4)_6\text{Cl}_2$	–	–	–	–	–	–	–	–	–	0.6533 Kreidler and Hummel 1970
$\text{Ba}_{10}(\text{AsO}_4)_6\text{Br}_2$	–	–	–	–	–	–	–	–	–	Not shown Manca et al. 1980
$\text{Ba}_{10}(\text{AsO}_4)_6\text{Cl}_2$	–	–	–	–	–	–	–	–	–	Not shown Chai 2020
$\text{Cd}_{10}(\text{AsO}_4)_6\text{OH}_2$	–	–	–	–	–	–	–	–	–	Not shown Manca et al. 1980
$\text{Cd}_{10}(\text{AsO}_4)_6\text{Cl}_2$	–	–	–	–	–	–	–	–	–	0.7348 Kreidler and Hummel 1970
$\text{Pb}_{10}(\text{AsO}_4)_6\text{F}_2$	–	–	–	–	–	–	–	–	–	0.7426 Chance 2014
$\text{Pb}_{10}(\text{AsO}_4)_6\text{OH}_2$	–	–	–	–	–	–	–	–	–	Not shown Manca et al. 1980
$\text{Pb}_{10}(\text{AsO}_4)_6\text{Cl}_2$	–	–	–	–	–	–	–	–	–	0.7470 Bell et al. 2008
$\text{Pb}_{10}(\text{AsO}_4)_6\text{Br}_2$	–	–	–	–	–	–	–	–	–	Not shown Manca et al. 1980
$\text{Pb}_{10}(\text{AsO}_4)_6\text{Cl}_2$	–	–	–	–	–	–	–	–	–	0.6551 Dunn and Rouse 1978
$\text{Ba}_{10}(\text{AsO}_4)_6\text{Br}_2$	–	–	–	–	–	–	–	–	–	Not shown Manca et al. 1980
$\text{Cd}_{10}(\text{AsO}_4)_6\text{F}_2$	–	–	–	–	–	–	–	–	–	Not shown Karbovskiy et al. 2011
$\text{Cd}_{10}(\text{AsO}_4)_6\text{OH}_2$	–	–	–	–	–	–	–	–	–	Not shown Karbovskiy et al. 2011
$\text{Cd}_{10}(\text{AsO}_4)_6\text{Cl}_2$	–	–	–	–	–	–	–	–	–	0.5589 Johnston et al. 2004
$\text{Cd}_{10}(\text{AsO}_4)_6\text{Br}_2$	–	–	–	–	–	–	–	–	–	Not shown Karbovskiy et al. 2011
$\text{Cd}_{10}(\text{AsO}_4)_6\text{Cl}_{1.6}(\text{OH})_{0.34}$	–	–	–	–	–	–	–	–	–	0.5689 Kreidler and Hummel 1970
$\text{Cd}_{10}(\text{AsO}_4)_6\text{Br}_2$	–	–	–	–	–	–	–	–	–	0.5609 Dordević et al. 2008
$\text{Pb}_{10}(\text{AsO}_4)_6\text{F}_2$	–	–	–	–	–	–	–	–	–	0.5759 Sudarsanan et al. 1977
$\text{Pb}_{10}(\text{AsO}_4)_6\text{Cl}_2$	–	–	–	–	–	–	–	–	–	0.6536 Sordyl et al. 2020

Table 1 (continued)

Chemical formula	$\Delta H_{\text{rel}}^{\circ}$ (kJ mol ⁻¹)	Reference	S° (J mol ⁻¹ K ⁻¹)	Référence	$C^{\circ}_{p, m}$ (J mol ⁻¹ K ⁻¹)	Référence	$\log K_{\text{sp}}$	Référence	V_m (nm ³)	Reference
$\text{Pb}_{10}(\text{AsO}_4)_6\text{OH}_2$										
$\text{Pb}_{10}(\text{AsO}_4)_6\text{OH}_{1.72}(\text{CO}_3)_{0.14}$	-6060	Puzio et al. 2022	-	Bajda 2010	-	-	-	Huang et al. 2014	0.6529	Kreidler and Hummel 1970
$\text{Pb}_{10}(\text{AsO}_4)_6\text{Cl}_2$	-5932	Bajda 2010	1315.0	Bajda 2010	-	-	-	Not shown	0.6679	ICDD 1997
									0.6710	Engel 1970
									0.6779	Sordyl et al. 2015
									0.6763	Antao and Dhaliwal 2018
									0.6779	Okudera 2013
							-152.6	Flis et al. 2011	0.6779	Flis et al. 2010
							-152.2	Flis et al. 2011	0.6779	Balkie et al. 2007
							-152.7	Bajda 2010	0.6776	Henderson et al. 2009
							-163.5	Liu et al. 2009	0.6778	
							-153.3	Bajda et al. 2007	0.6780	Henderson et al. 2009
							-170.8	Ingebenebor et al. 1989	0.6700	Dai et al. 1991
									0.6782	Calos and Kenneth 1990
									0.6612	Mayer et al. 1979
									0.6792	Merker and Wondratschek 1959
									0.6693	ICDD 1997
									0.6770	Sordyl et al. 2020
									0.6876	Merker and Wondratschek 1959
									0.6883	Sordyl et al. 2020
									0.6991	Sordyl et al. 2020
									0.7022	Merker and Wondratschek 1957
									0.5534	Pekov et al. 2021 (in press)
									0.5725	Dong and White 2004

Table 1 (continued)

Chemical formula	$\Delta H_{\text{rel}}^{\circ}$ (kJ mol ⁻¹)	Reference	S° (J mol ⁻¹ K ⁻¹)	Reference	$C^{\circ}_{p, m}$ Référence (J mol ⁻¹ K ⁻¹)	$\log K_{\text{sp}}$	Reference	V_m (nm ³)	Reference
$\text{Ca}_{10}(\text{VO}_4)_6\text{OH}_2$	–	–	–	–	–	–	–	–	Kreidler and Hummel 1970
$\text{Ca}_{10}(\text{VO}_4)_6\text{Cl}_2$	–	–	–	–	–	–	–	–	Not shown Karbovsky and Soroka 2014
$\text{Ca}_{10}(\text{VO}_4)_6\text{Br}_2$	–	–	–	–	–	–	–	–	Getman et al. 2001
$\text{Sr}_{10}(\text{VO}_4)_6\text{F}_2$	–	–	–	–	–	–	–	–	Beck et al. 2006
$\text{Sr}_{10}(\text{VO}_4)_6\text{OH}_2$	–	–	–	–	–	–	–	–	Kreidler and Hummel 1970
$\text{Sr}_{10}(\text{VO}_4)_6\text{Cl}_2$	–	–	–	–	–	–	–	–	Baran 1972
$\text{Sr}_{10}(\text{VO}_4)_6\text{Br}_2$	–	–	–	–	–	–	–	–	Knyazev et al. 2015
$\text{Ba}_{10}(\text{VO}_4)_6\text{OH}_2$	–	–	–	–	–	–	–	–	Zhang et al. 2015
$\text{Ba}_{10}(\text{VO}_4)_6\text{F}_2$	–	–	–	–	–	–	–	–	ICDD 2004
$\text{Ba}_{10}(\text{VO}_4)_6\text{Cl}_2$	–	–	–	–	–	–	–	–	Grisafe and Hummel 1970
$\text{Ba}_{10}(\text{VO}_4)_6\text{Br}_2$	–	–	–	–	–	–	–	–	Getman et al. 2007
						–	–	–	not seen Marchenko and Getman 2003
						–	–	–	Mayer et al. 1979
						–	–	–	Knyazev et al. 2015
						–	–	–	Beck et al. 2006
						–	–	–	ICDD 2004
						–	–	–	Grisafe and Hummel 1970
						–	–	–	Baran 1972
						–	–	–	Chai 2020
						–	–	–	ICDD 2004
						–	–	–	Not shown Krause 1955
						–	–	–	0.7460 Beck et al. 2006
						–	–	–	Roh and Hong 2005
						–	–	–	ICDD 2004
						–	–	–	0.7494

Table 1 (continued)

Chemical formula	$\Delta H_{\text{rel}}^{\circ}$ (kJ mol ⁻¹)	Reference	S° (J mol ⁻¹ K ⁻¹)	Référence	$C^{\circ}_{p, m}$ (J mol ⁻¹ K ⁻¹)	Référence	$\log K_{\text{sp}}$	Référence	V_m (nm ³)	Référence
$\text{Ba}_{10}(\text{VO}_4)_6\text{Br}_2$	–	–	–	–	–	–	–	–	0.7555	Baran 1972
$\text{Cd}_{10}(\text{VO}_4)_6\text{F}_2$	–	–	–	–	–	–	–	–	0.5381	Karbovsky et al. 2014
$\text{Cd}_{10}(\text{VO}_4)_6\text{OH}_2$	–	–	–	–	–	–	–	–	0.5596	Karbovsky et al. 2014
$\text{Cd}_{10}(\text{VO}_4)_6\text{Cl}_2$	–	–	–	–	–	–	–	–	0.5798	Chernorukov et al. 2011
$\text{Cd}_{10}(\text{VO}_4)_6\text{Br}_2$	–	–	–	–	–	–	–	–	0.5689	Karbovsky et al. 2014
$\text{Cd}_{10}(\text{VO}_4)_6\text{I}_2$	–	–	–	–	–	–	–	–	0.5854	Sudarsanan et al. 1977
$\text{Pb}_{10}(\text{VO}_4)_6\text{F}_2$	–	–	–	–	–	–	–	–	0.5976	Sudarsanan et al. 1977
$\text{Pb}_{10}(\text{VO}_4)_6\text{OH}_2$	–	–	–	–	–	–	–	–	0.6510	Oka et al. 2022
$\text{Pb}_{10}(\text{VO}_4)_6\text{Cl}_2$	–	–	–	–	–	–	–	–	Not shown	Nakamura et al. 2020
$\text{Pb}_{10}(\text{VO}_4)_6\text{Br}_2$	–	–	–	–	–	–	–	–	0.6497	Kreidler and Hummel 1970
$\text{Pb}_{10}(\text{VO}_4)_6\text{I}_2$	–	–	–	–	–	–	–	–	0.6532	Grisafe and Hum- mel 1970
$\text{Pb}_{10}(\text{VO}_4)_6\text{OH}_2$	–	–	–	–	–	–	–	–	0.6484	Merker and Won- dratschek 1957
$\text{Pb}_{10}(\text{VO}_4)_6\text{Cl}_2$	–7592	Puzio et al. 2021	–	Puzio et al. 2021	–	–	–	–	0.6677	Engel 1970
$\text{Pb}_{10}(\text{VO}_4)_6\text{Br}_2$	–7338	Chernorukov et al. 2010	1334.0	Chernorukov et al. 2010	867.4	Chernorukov et al. 2010	–183.8	Topolska et al. 2021	Not shown	Nakamura et al. 2020
$\text{Pb}_{10}(\text{VO}_4)_6\text{I}_2$	–	–	–	–	–	–	–172.0	Gerke et al. 2009	0.6761	Antao and Dhali- wal 2018
$\text{Pb}_{10}(\text{VO}_4)_6\text{OH}_2$	–	–	–	–	–	–	–	–	0.6774	Solecka et al. 2018
$\text{Pb}_{10}(\text{VO}_4)_6\text{Cl}_2$	–	–	–	–	–	–	–	–	0.6771	Okudera 2013
$\text{Pb}_{10}(\text{VO}_4)_6\text{Br}_2$	–	–	–	–	–	–	–	–	0.6777	Chernorukov et al. 2011
$\text{Pb}_{10}(\text{VO}_4)_6\text{I}_2$	–	–	–	–	–	–	–	–	0.6727	Chernorukov et al. 2010
$\text{Pb}_{10}(\text{VO}_4)_6\text{OH}_2$	–	–	–	–	–	–	–	–	0.6787	Trotter and Barnes 1958
$\text{Pb}_{10}(\text{VO}_4)_6\text{Cl}_2$	–	–	–	–	–	–	–	–	0.6761	Merker and Won- dratschek 1957

Table 1 (continued)

Chemical formula	$\Delta H^\circ_{\text{rel}}$ (kJ mol ⁻¹)	Reference	S° (J mol ⁻¹ K ⁻¹)	Reference	$C^{\circ}_{\text{p}, \text{m}}$ (J mol ⁻¹ K ⁻¹)	Reference	$\log K_{\text{sp}}$	Reference	V_m (nm ³)	Reference
Pb ₁₀ (VO ₄) ₆ Br ₂	–	–	–	–	–	–	–	–	–	Nakamura et al. 2020
Pb _{9.85} (VO ₄) ₆ I _{1.7}	–	–	–	–	–	–	–	–	–	Merker and Won- dratschek 1957
Pb ₁₀ (VO ₄) ₆ I ₂	–5436	Fleche 2002	1359.5	Fleche 2002	877.8	Fleche 2002	0.6881	0.7025	0.7001	Audubert et al. 1999

Note: $\Delta H^\circ_{\text{rel}}$ – enthalpy of formation from elements; S° – standard entropy; $C^{\circ}_{\text{p}, \text{m}}$ – heat capacity; $\log K_{\text{sp}}$ – logarithm of solubility constant for given dissolution reaction: $M_{\text{e},10}(\text{AO}_4)_6X_2 \leftrightarrow 10\text{Me}^{2+} + 6\text{AO}_4^{3-} + 2X^-$; ICDD—International Center for Diffraction Data (PDF 1997) and PDF-2 (2004) database; **bold** – selected experimental values used in calculations below

Ca₁₀(PO₄)₆X₂. The correlation of $\Delta H^\circ_{\text{f,el}}$ of apatites with molar volume of apatite (V_m) is also apparent (Fig. 1B). So far, such relationships can be found within P-apatites. Gaps in experimental data do not allow a complete picture of these relationships for As- or V-apatites.

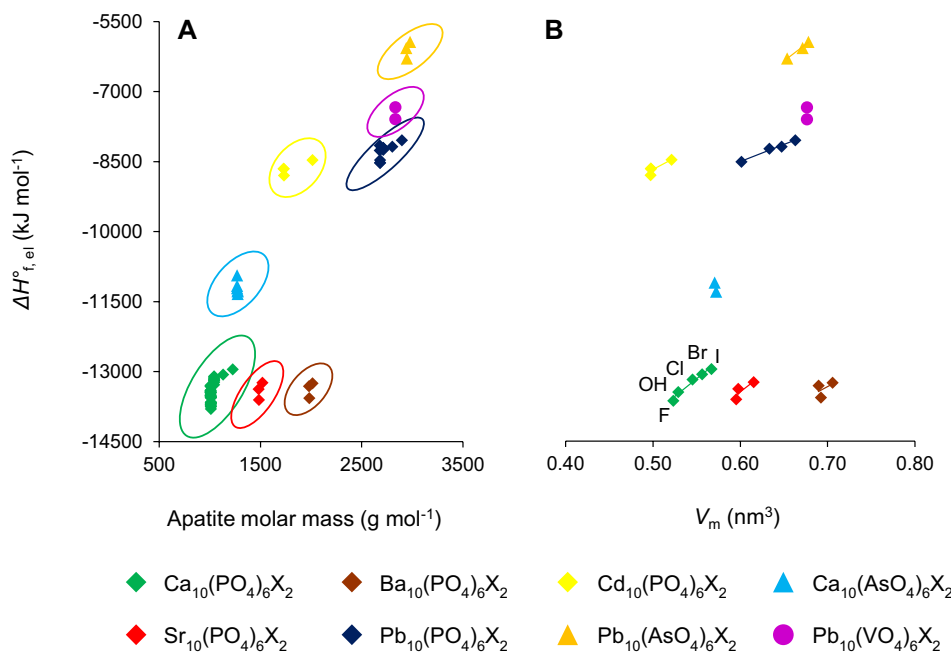
Correlation of V_m with ionic radius of halogen anion X

The molar volume V_m is not yet known for all apatites e.g., Ca₁₀(VO₄)₆I₂, Cd₁₀(AsO₄)₆I₂ or Ba₁₀(AsO₄)₆Br₂ (Table 1). Glasser and Jenkins have proposed a method to calculate missing V_m values based on the sum of contributions of internally consistent single-ion volumes (Jenkins and Glasser [2003](#); Glasser and Jenkins [2008](#)). The use of their method gives promising and accurate results with the uncertainty not exceeding $\pm 11\%$ compare to experimental V_m (Glasser and Jenkins [2008](#)). Over the last 15 years, many of the experimental diffraction data have been published for not only phosphate but also arsenate and vanadate apatites. This allows the calculation of more experimental V_m values and verification of this approach.

In this work, we propose a different procedure for predicting V_m values for apatites whose structure has not yet been determined or for potential apatite-based structures predicted by Wang ([2015](#)) and Hartnett et al. ([2019](#)). The method is based on the linear correlation of the V_m value with the ionic radius (R_i) of the halides present at the X position (Fig. 2). In this procedure, all available experimental data of apatites and their synthetic analogs (*exptlV_m*) are divided into apatite subgroups based on the same substitution at Me²⁺ and AO₄³⁻ positions but different X. The subgroups should be considered separately within the X substitutions excluding OH (X=F, Cl, Br, I), e.g., Ca₁₀(PO₄)₆X₂, Pb₁₀(PO₄)₆X₂, Ca₁₀(AsO₄)₆X₂, Pb₁₀(AsO₄)₆X₂, Ca₁₀(VO₄)₆X₂, Pb₁₀(VO₄)₆X₂, etc. A complete dataset within apatite subgroups exists for the Pb₁₀(AsO₄)₆X₂, Pb₁₀(VO₄)₆X₂ and Cd₁₀(VO₄)₆X₂ (Fig. 2). Both visual inspection and Pearson correlation coefficient along with R² values greater than 0.99 indicate positive linear correlations. This positive correlation of V_m vs. R_i allows for interpolation and extrapolation within other apatite subgroups. Linear correlation was assumed for all apatite subgroups based on linearity within subgroups with the most available experimental data. If there are at least two known values of *exptlV_m* within a subgroup, the parameters a and b of the linear regression between *exptlV_m* and R_i of the halides can be calculated. The unknown values of V_m are predicted from the relationship (determined separately for each subgroup of apatites):

$$\text{pred}V_m = a \times R_i + b \quad (1)$$

Fig. 1 A Plot of the experimental enthalpies of formation from elements ($\Delta H_{f,\text{el}}^\circ$) against molar mass of selected apatites showing the presence of populations (subgroups). B Example of a systematic relationship between $\Delta H_{f,\text{el}}^\circ$ and V_m (based on arithmetic means of $\Delta H_{f,\text{el}}^\circ$ values compiled in Table 1)



where $\text{pred}V_m$ is predicted molar volume of apatite and R_i is the ionic radius of element X (X=F⁻, Cl⁻, Br⁻, and I⁻; Table SI 1). Linear regression coefficients a and b are listed in Table SI 2. The results of calculations are presented in Fig. 2 as empty marks. Predicted molar volumes ($\text{pred}V_m$) are summarized in Table 2. These volumes will be used in calculations below as data equal to the experimental ones.

A comparison of the values obtained using the approach presented here ($\text{pred}V_m$) with those obtained using the Glasser–Jenkins (2008) method ($\text{calc}V_m$) and with the experimental values is presented in Table 2. Precision of prediction was estimated by the relative percentage difference. The difference between $\text{exptl}V_m$ and the same values calculated from the regression does not exceed 0.5% for any apatite considered. In contrast, the differences determined for the values calculated by the Glasser–Jenkins method are up to 10% for calcium phosphate apatites, 30% for lead phosphate apatites, or 20% for cadmium phosphate apatites. This large difference is partly because the volumes used by Glasser and Jenkins (2008) for Pb²⁺ and Cd²⁺ cations were not corrected (calibrated) but taken directly from Marcus (1987). This indicates that greater precision in predicting V_m values was achieved using the approach presented in this work.

Correlation of lattice energy U_{POT} with V_m

U_{POT} is the energy change upon the formation of one mole of an ionic compound from its constituent ions in the gaseous state. Experimental lattice energy ($\text{exptl}U_{\text{POT}}$) can be determined using Born–Haber thermochemical cycles described in detail by Flora et al. (2004b). For those apatites for which experimentally determined $\Delta H_{f,\text{el}}^\circ$ is available, the $\text{exptl}U_{\text{POT}}$

values are summarized in Table 3. The thermochemical data necessary to determine $\text{exptl}U_{\text{POT}}$ are given in Table SI 3.

The lattice energies listed as $\text{exptl}U_{\text{POT}}$ in Table 3 were obtained from the lattice enthalpy ΔH_{latt} by correcting for the difference between enthalpy and lattice energy U_{POT} (Jenkins 2005). ΔH_{latt} involves correction of the U_{POT} term by an appropriate RT (where R is the gas constant and T is the temperature in K; Jenkins and Lieberman 2005). For U_{POT} extraction from the Born–Fajans–Haber cycle (which is essentially an enthalpy-based thermochemical cycle) the ΔH_{latt} must be transformed using an extension discussed by Jenkins et al. 1999. Finally, for F-, Cl-, Br- and I-apatites, $\Delta H_{\text{latt}} = U_{\text{POT}}$, so we do not present ΔH_{latt} values separately (Jenkins et al. 1999).

Lattice energy can be calculated also as $\text{calc}U_{\text{POT}}$ using the improved Kapustinskii equation, a generalized version of which was given by Glasser and Jenkins (2000). This equation for an isostructural family of minerals requires no parameters other than the molar volume V_m (in nm³) and is reduced to the form:

$$\text{calc}U_{\text{POT}} \left(\frac{\text{kJ}}{\text{mol}} \right) = \frac{26680}{\sqrt[3]{V_m}} \quad (2)$$

Flora et al. (2004b) used this equation to calculate $\text{calc}U_{\text{POT}}$ values for phosphate apatites. We have extended these calculations to As- and V-apatites using both experimental and predicted V_m (Table 3). The results are presented in Table 3 ($\text{calc}U_{\text{POT}}$) and in Fig. 3. The values calculated based on Eq. (2) differ both from $\text{exptl}U_{\text{POT}}$ and from intuitively expected numbers. The U_{POT} value depends not only on the morphology and distribution of the individual atoms

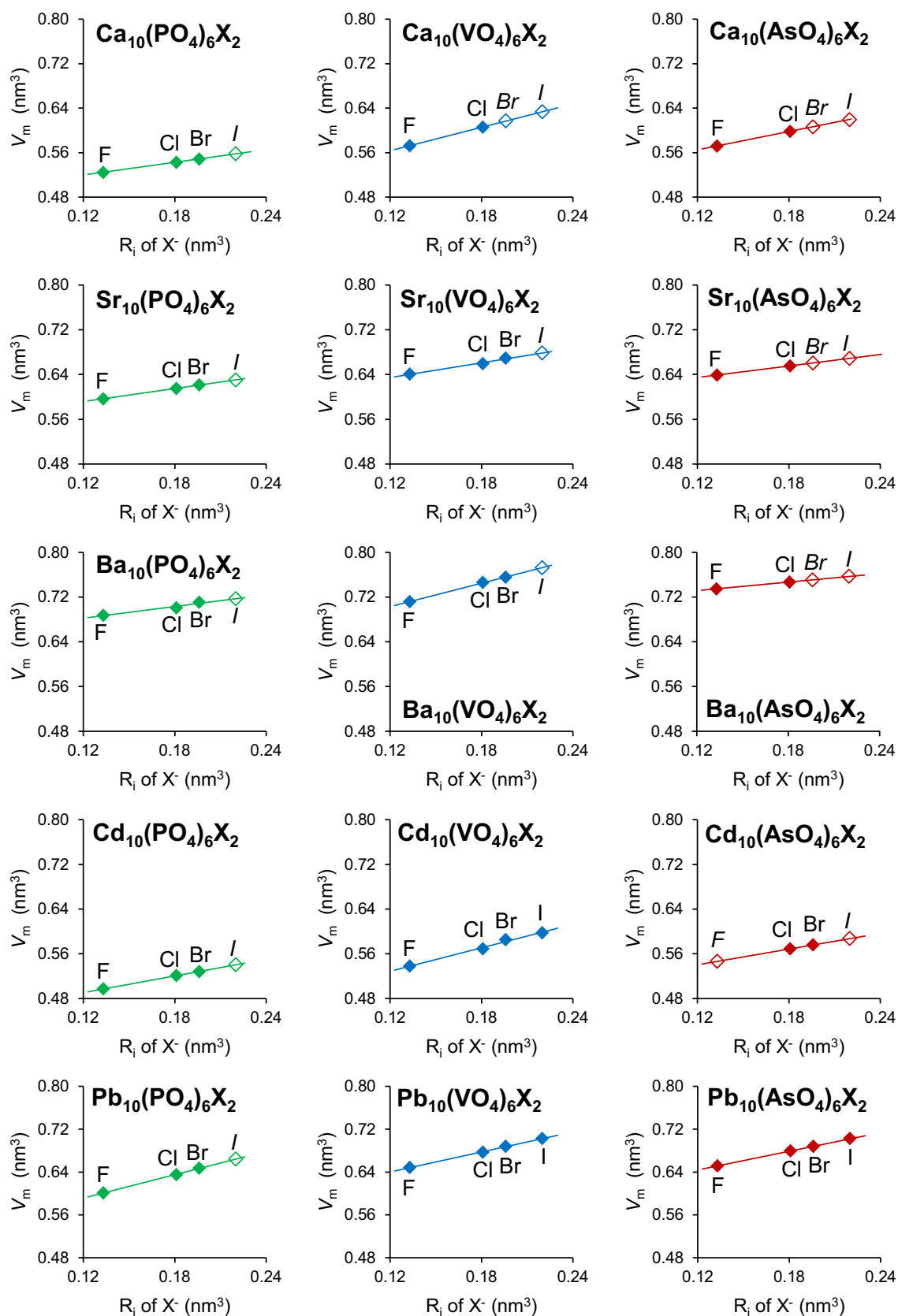


Fig. 2 Correlation of V_m with the ionic radius of halogen X^- for selected apatite subgroups. Experimental data used for regression are plotted as solid marks. Values predicted based on the Eq. 1 are plotted as open symbols

Table 2 Comparison of the experimental molar volumes with values calculated based on Glasser and Jenkins (2008) and values predicted in this work

Apatite	exptIV _m or predV _m (nm ³)	calcV _m (nm ³)	% diff ¹	predV _m (nm ³)	% diff ²
Ca ₁₀ (PO ₄) ₆ F ₂	0.5246	0.5710	-9	0.5246	-0.0023
Ca ₁₀ (PO ₄) ₆ Cl ₂	0.5430	0.6026	-11	0.5429	0.0095
Ca ₁₀ (PO ₄) ₆ Br ₂	0.5486	0.6156	-12	0.5487	-0.0072
Ca ₁₀ (PO ₄) ₆ I ₂	0.5578	0.6406	-15	0.5578	0.0000
Sr ₁₀ (PO ₄) ₆ F ₂	0.5967	0.5830	2	0.5967	0.0052
Sr ₁₀ (PO ₄) ₆ Cl ₂	0.6152	0.6146	0	0.6153	-0.0211
Sr ₁₀ (PO ₄) ₆ Br ₂	0.6213	0.6276	-1	0.6212	0.0159
Sr ₁₀ (PO ₄) ₆ I ₂	0.6305	0.6526	-4	0.6305	0.0000
Ba ₁₀ (PO ₄) ₆ F ₂	0.6874	0.6400	7	0.6868	0.0933
Ba ₁₀ (PO ₄) ₆ Cl ₂	0.7008	0.6716	4	0.7035	-0.3843
Ba ₁₀ (PO ₄) ₆ Br ₂	0.7107	0.6846	4	0.7087	0.2887
Ba ₁₀ (PO ₄) ₆ I ₂	0.7170	0.7096	1	0.7170	0.0000
Cd ₁₀ (PO ₄) ₆ F ₂	0.4970	0.4160	16	0.4970	-0.0096
Cd ₁₀ (PO ₄) ₆ Cl ₂	0.5211	0.4476	14	0.5209	0.0385
Cd ₁₀ (PO ₄) ₆ Br ₂	0.5282	0.4606	13	0.5284	-0.0289
Cd ₁₀ (PO ₄) ₆ I ₂	0.5403	0.4856	10	0.5403	0.0000
Pb ₁₀ (PO ₄) ₆ F ₂	0.6010	0.4660	22	0.6008	0.0286
Pb ₁₀ (PO ₄) ₆ Cl ₂	0.6350	0.4976	22	0.6357	-0.1136
Pb ₁₀ (PO ₄) ₆ Br ₂	0.6472	0.5106	21	0.6467	0.0849
Pb ₁₀ (PO ₄) ₆ I ₂	0.6641	0.5356	19	0.6641	0.0000
Ca ₁₀ (AsO ₄) ₆ F ₂	0.5721	0.6238	-9	0.5721	0.0000
Ca ₁₀ (AsO ₄) ₆ Cl ₂	0.5984	0.6554	-10	0.5984	0.0000
Ca ₁₀ (AsO ₄) ₆ Br ₂	0.6066	0.6684	-10	0.6066	0.0000
Ca ₁₀ (AsO ₄) ₆ I ₂	0.6198	0.6934	-12	0.6198	0.0000
Sr ₁₀ (AsO ₄) ₆ F ₂	0.6392	0.6358	1	0.6392	0.0000
Sr ₁₀ (AsO ₄) ₆ Cl ₂	0.6556	0.6674	-2	0.6556	0.0000
Sr ₁₀ (AsO ₄) ₆ Br ₂	0.6607	0.6804	-3	0.6607	0.0000
Sr ₁₀ (AsO ₄) ₆ I ₂	0.6690	0.7054	-5	0.6690	0.0000
Ba ₁₀ (AsO ₄) ₆ F ₂	0.7348	0.6928	6	0.7348	0.0000
Ba ₁₀ (AsO ₄) ₆ Cl ₂	0.7470	0.7244	3	0.7470	0.0000
Ba ₁₀ (AsO ₄) ₆ Br ₂	0.7508	0.7374	2	0.7508	0.0000
Ba ₁₀ (AsO ₄) ₆ I ₂	0.7569	0.7624	-1	0.7569	0.0000
Cd ₁₀ (AsO ₄) ₆ F ₂	0.5465	0.4688	14	0.5465	0.0000
Cd ₁₀ (AsO ₄) ₆ Cl ₂	0.5689	0.5004	12	0.5689	0.0000
Cd ₁₀ (AsO ₄) ₆ Br ₂	0.5759	0.5134	11	0.5759	0.0000
Cd ₁₀ (AsO ₄) ₆ I ₂	0.5871	0.5384	8	0.5871	0.0000
Pb ₁₀ (AsO ₄) ₆ F ₂	0.6516	0.5188	20	0.6515	0.0214
Pb ₁₀ (AsO ₄) ₆ Cl ₂	0.6792	0.5504	19	0.6793	-0.0119
Pb ₁₀ (AsO ₄) ₆ Br ₂	0.6876	0.5634	18	0.6880	-0.0544
Pb ₁₀ (AsO ₄) ₆ I ₂	0.7022	0.5884	16	0.7019	0.0449
Ca ₁₀ (VO ₄) ₆ F ₂	0.5725	0.6268	-9	0.5725	0.0000
Ca ₁₀ (VO ₄) ₆ Cl ₂	0.6062	0.6584	-9	0.6062	0.0000
Ca ₁₀ (VO ₄) ₆ Br ₂	0.6167	0.6714	-9	0.6167	0.0000
Ca ₁₀ (VO ₄) ₆ I ₂	0.6335	0.6964	-10	0.6335	0.0000
Sr ₁₀ (VO ₄) ₆ F ₂	0.6408	0.6388	0	0.6403	0.0768
Sr ₁₀ (VO ₄) ₆ Cl ₂	0.6593	0.6704	-2	0.6614	-0.3134
Sr ₁₀ (VO ₄) ₆ Br ₂	0.6695	0.6834	-2	0.6679	0.2351
Sr ₁₀ (VO ₄) ₆ I ₂	0.6785	0.7084	-4	0.6785	0.0000
Ba ₁₀ (VO ₄) ₆ F ₂	0.7118	0.6958	2	0.7119	-0.0181
Ba ₁₀ (VO ₄) ₆ Cl ₂	0.7460	0.7274	2	0.7455	0.0726

Table 2 (continued)

Apatite	exptlV_m or <i>predV_m</i> (nm ³)	calcV _m (nm ³)	% diff ¹	<i>predV_m</i> (nm ³)	% diff ²
Ba ₁₀ (VO ₄) ₆ Br ₂	0.7555	0.7404	2	0.7559	-0.0546
Ba ₁₀ (VO ₄) ₆ I ₂	0.7727	0.7654	1	0.7727	0.0000
Cd ₁₀ (VO ₄) ₆ F ₂	0.5381	0.4718	12	0.5379	0.0384
Cd ₁₀ (VO ₄) ₆ Cl ₂	0.5689	0.5034	12	0.5715	-0.4589
Cd ₁₀ (VO ₄) ₆ Br ₂	0.5854	0.5164	12	0.5820	0.5966
Cd ₁₀ (VO ₄) ₆ I ₂	0.5976	0.5414	9	0.5987	-0.1823
Pb ₁₀ (VO ₄) ₆ F ₂	0.6484	0.5218	20	0.6482	0.0370
Pb ₁₀ (VO ₄) ₆ Cl ₂	0.6771	0.5534	18	0.6781	-0.1415
Pb ₁₀ (VO ₄) ₆ Br ₂	0.6881	0.5664	18	0.6874	0.0997
Pb ₁₀ (VO ₄) ₆ I ₂	0.7024	0.5914	16	0.7024	0.0045

Note: **exptlV_m** – experimental data extracted from Table 1; calcV_m – based on Glasser and Jenkins (2008); *predV_m* – based on Eq. 1; %diff¹=100 · (exptlV_m - calcV_m) / exptlV_m; %diff²=100 · (exptlV_m - predV_m) / exptlV_m; the data in the first column will be used in further calculations

Table 3 Comparison of the experimental lattice energies with values calculated using the improved Kapustinskii equation (Flora et al. 2004b) and values predicted in this work

Apatite	exptlU_{POT} or <i>predU_{POT}</i> (kJ mol ⁻¹)	calcU _{POT} (kJ mol ⁻¹)	% diff ¹	<i>predU_{POT}</i> (kJ mol ⁻¹)	% diff ²
Ca ₁₀ (PO ₄) ₆ F ₂	34,158	33,080	3	34,160	-0.01
Ca ₁₀ (PO ₄) ₆ Cl ₂	33,865	32,703	4	33,856	0.03
Ca ₁₀ (PO ₄) ₆ Br ₂	33,756	32,591	4	33,763	-0.02
Ca ₁₀ (PO ₄) ₆ I ₂	33,611	32,411	4	33,611	0.00
Sr ₁₀ (PO ₄) ₆ F ₂	32,837	31,691	3	32,837	0.00
Sr ₁₀ (PO ₄) ₆ Cl ₂	32,516	31,370	4	32,516	0.00
Sr ₁₀ (PO ₄) ₆ Br ₂	32,411	31,268	4	32,411	0.00
Sr ₁₀ (PO ₄) ₆ I ₂	32,251	31,114	4	32,251	0.00
Ba ₁₀ (PO ₄) ₆ F ₂	31,372	30,231	4	31,372	0.00
Ba ₁₀ (PO ₄) ₆ Cl ₂	31,104	30,037	4	31,104	0.00
Ba ₁₀ (PO ₄) ₆ Br ₂	30,905	29,896	4	30,905	0.00
Ba ₁₀ (PO ₄) ₆ I ₂	30,779	29,809	3	30,779	0.00
Cd ₁₀ (PO ₄) ₆ F ₂	36,408	33,682	7	36,408	0.00
Cd ₁₀ (PO ₄) ₆ Cl ₂	36,126	33,155	8	36,126	0.00
Cd ₁₀ (PO ₄) ₆ Br ₂	36,043	33,006	8	36,043	0.00
Cd ₁₀ (PO ₄) ₆ I ₂	35,902	32,758	9	35,902	0.00
Pb ₁₀ (PO ₄) ₆ F ₂	33,603	31,615	6	33,600	0.01
Pb ₁₀ (PO ₄) ₆ Cl ₂	33,435	31,040	7	33,445	-0.03
Pb ₁₀ (PO ₄) ₆ Br ₂	33,397	30,844	8	33,389	0.02
Pb ₁₀ (PO ₄) ₆ I ₂	33,312	30,580	8	33,312	0.00

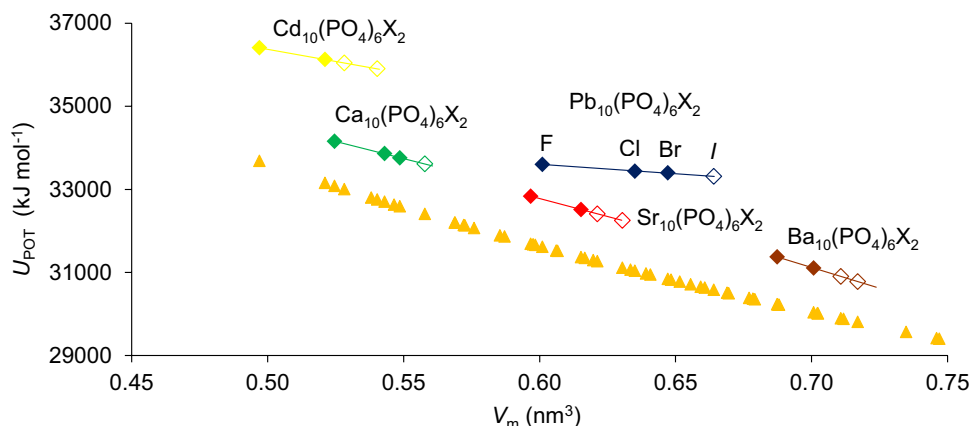
Note: %diff¹=100 · (exptlU_{POT} - calcU_{POT}) / exptlU_{POT}; %diff²=100 · (exptlU_{POT} - predU_{POT}) / exptlU_{POT}; the data from the first column will be used in further calculations

in the structure but also to a large extent on the chemical nature of these atoms, which is not included in the calculations. For example, for the apatite pair Ca₁₀(PO₄)₆F₂ and Cd₁₀(PO₄)₆Cl₂, the experimentally determined exptlU_{POT} values are 17,124 and 18,063 kJ mol⁻¹, respectively. However, since the difference in exptlV_m for these end-members is small (on the order of 0.4%), the calcU_{POT} values determined for these apatites from Eq. (2) are 16,554 and 16,577 kJ mol⁻¹, respectively. Not only do these values

deviate significantly from experimental determinations, but they are also almost indistinguishable from one another. This is, among other things, an artifact of using the molar volume V_m as the only variable in Eq. (2).

In contrast, the plot of exptlU_{POT} against V_m shows that there is a linear relationship between them within the distinct apatite subgroups (Fig. 3). The different slopes of the trend lines show the varying effect of the halogen on the thermochemical behavior for apatite subgroups. Some apatites have

Fig. 3 Correlation of U_{POT} with V_m for selected phosphate apatite subgroups. A row of stars represents values of $\text{calc}U_{\text{POT}}$ estimated using Eq. 2. Values predicted using the Eq. 3 are open symbols



very similar molar volumes but completely different chemical compositions. The linear correlations shown in Fig. 3 can be used for interpolation and extrapolation to predict missing U_{POT} values. The steps in determining U_{POT} and the prediction process are similar to the prediction of V_m . The $\text{exptl}U_{\text{POT}}$ data of apatites and their synthetic analogs should be divided into apatite subgroups. The subgroups should be considered separately within the X substitutions excluding OH ($X=F, \text{Cl}, \text{Br}, \text{I}$), e.g., $\text{Ca}_{10}(\text{PO}_4)_6\text{X}_2$, $\text{Pb}_{10}(\text{PO}_4)_6\text{X}_2$, $\text{Ca}_{10}(\text{AsO}_4)_6\text{X}_2$, $\text{Pb}_{10}(\text{AsO}_4)_6\text{X}_2$, $\text{Ca}_{10}(\text{VO}_4)_6\text{X}_2$, $\text{Pb}_{10}(\text{VO}_4)_6\text{X}_2$, etc. If there are at least two known values of $\text{exptl}U_{\text{POT}}$ within a subgroup, the parameters a and b of the linear regression between $\text{exptl}U_{\text{POT}}$ and the molar volume V_m are calculated. Lattice energy $\text{pred}U_{\text{POT}}$ is predicted from the equation:

$$\text{pred}U_{\text{POT}} = a \times V_m + b \quad (3)$$

The $\text{pred}U_{\text{POT}}$ values obtained by this method are plotted in Fig. 3 as empty marks. Linear regression coefficients a and b along with Pearson coefficient R and R^2 are listed in Table SI 4. A comparison of the $\text{pred}U_{\text{POT}}$ values and $\text{calc}U_{\text{POT}}$ obtained using Eq. (2) with the experimental values shows that greater precision in predicting U_{POT} values was achieved (as assessed by the relative percentage deviation from experimental data). The difference between $\text{exptl}U_{\text{POT}}$ and the values calculated from the regression does not exceed 0.05% for any apatite considered. In contrast, the differences calculated using the values computed by the Glasser–Jenkins (2000) method are up to 4% for calcium phosphate apatites, 8% for lead phosphate apatites, or 9% for cadmium phosphate apatites. All the $\text{pred}U_{\text{POT}}$ values summarized in Table 3 will be used in further calculations below on par with the experimental data.

Prediction of $\Delta H^\circ_{\text{f,el}}$ using U_{POT}

Figure 4 shows examples of the linear correlation of $\Delta H^\circ_{\text{f,el}}$ of apatites as a function of U_{POT} for selected phosphate

apatites. The linearity of these correlations is enforced by the Born–Haber cycle. Phosphate apatites were chosen to present these correlations. This is currently impossible for As- and V-apatites due to the lack of data. Using all the $\text{exptl}U_{\text{POT}}$ and the $\text{pred}U_{\text{POT}}$ calculated from Eq. 3, the $\text{pred}\Delta H^\circ_{\text{f,el}}$ can be determined by extrapolating the linear relationships shown in Fig. 4:

$$\text{pred}\Delta H^\circ_{\text{f,el}} = a \times U_{\text{POT}} + b \quad (4)$$

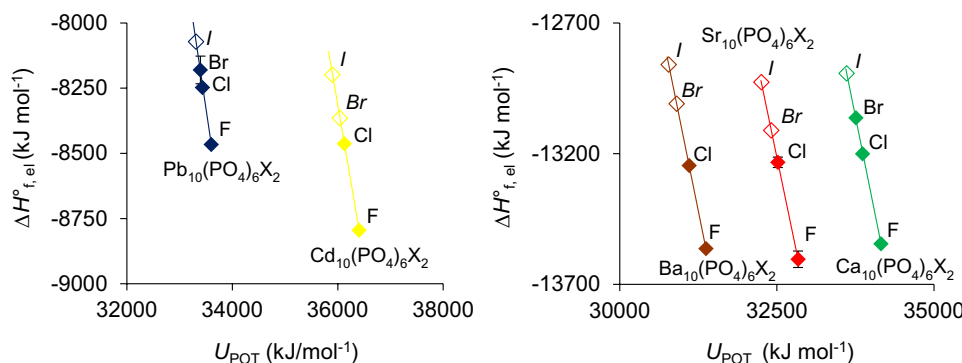
The linear regression coefficients given in Table SI 5 were used for the calculations according to Eq. 4. The values obtained by this method are plotted in Fig. 4 as empty marks. A comparison of the $\text{pred}\Delta H^\circ_{\text{f,el}}$ with the experimental ones is shown in Table 4. The discrepancies do not exceed 0.1% relative error. This correlation allowed the prediction of eight, so far unknown, $\Delta H^\circ_{\text{f,el}}$ values for the following end-members: $\text{Ca}_{10}(\text{PO}_4)_6\text{L}_2$, $\text{Sr}_{10}(\text{PO}_4)_6\text{Br}_2$, $\text{Sr}_{10}(\text{PO}_4)_6\text{I}_2$, $\text{Ba}_{10}(\text{PO}_4)_6\text{Br}_2$, $\text{Ba}_{10}(\text{PO}_4)_6\text{I}_2$, $\text{Cd}_{10}(\text{PO}_4)_6\text{Br}_2$, $\text{Cd}_{10}(\text{PO}_4)_6\text{I}_2$, and $\text{Pb}_{10}(\text{PO}_4)_6\text{I}_2$.

Prediction of $\Delta H^\circ_{\text{f,el}}$ of apatites using $\Delta H^\circ_{\text{f,el}}$ of X^-

The correlations of $\Delta H^\circ_{\text{f,el}}$ with $\text{exptl}U_{\text{POT}}$ do not allow the prediction of missing $\Delta H^\circ_{\text{f,el}}$ for As- and V-apatites even in the case when $\Delta H^\circ_{\text{f,el}}$ is available: the enthalpy of formation of the gaseous AsO_4^{3-} and VO_4^{3-} ions is still unknown, making it impossible to determine $\text{exptl}U_{\text{POT}}$ using Born–Haber cycles. Moreover, “ab initio” calculations are also not feasible due to the structural complexity of these particular apatites. To address this issue, we explored a linear relationship between $\Delta H^\circ_{\text{f,el}}$ of apatite and $\Delta H^\circ_{\text{f,el}}$ of monovalent anion X^- .

The experimental $\Delta H^\circ_{\text{f,el}}$ from Table 1 and the predictions from Table 4 were used to plot these relationships (Fig. 5). In addition to halides, the OH^- anion and OH -apatites were used because they fit the linear trends with $R^2 > 0.99$ (except

Fig. 4 Correlation of $\Delta H_{f,\text{el}}^\circ$ with U_{POT} (from the first column in Table 3) within apatite subgroups used for prediction of missing $\Delta H_{f,\text{el}}^\circ$. Values predicted using the Eq. 4 are plotted as open symbols. Error bars from literature where available



for $\text{Ba}_{10}(\text{PO}_4)_6\text{X}_2$ where $R^2=0.97$; Table SI 6). The extrapolation of the regression lines allowed to obtain a prediction of $\Delta H_{f,\text{el}}^\circ$ for calcium and lead As-apatites. For calculation of predicted $\Delta H_{f,\text{el}}^\circ$ from the equation:

$$\text{pred}\Delta H_{f,\text{el}}^\circ = a \times \Delta H_{f,\text{el}}^\circ \text{ of } X^- + b \quad (5)$$

The $\Delta H_{f,\text{el}}^\circ$ of X^- from Table SI 1 and linear correlation coefficients from Table SI 6 were used. The existing and predicted $\Delta H_{f,\text{el}}^\circ$ data are compared in Table 5. The difference

between $\text{exptl}\Delta H_{f,\text{el}}^\circ$ and the values calculated from the regression does not exceed 0.27% for any apatite considered. The $\Delta H_{f,\text{el}}^\circ$ values were predicted for the following apatites: $\text{Ca}_{10}(\text{AsO}_4)_6\text{Cl}_2$, $\text{Ca}_{10}(\text{AsO}_4)_6\text{Br}_2$, $\text{Ca}_{10}(\text{AsO}_4)_6\text{I}_2$, $\text{Pb}_{10}(\text{AsO}_4)_6\text{Br}_2$, and $\text{Pb}_{10}(\text{AsO}_4)_6\text{I}_2$. Linear extrapolation from only two points was used for $\text{Ca}_{10}(\text{AsO}_4)_6\text{X}_2$. The linear correlation was assumed based on the linearity within other apatite subgroups.

Prediction of $\Delta H_{f,\text{el}}^\circ$ of apatites using $\Delta H_{f,\text{el}}^\circ$ of AO_4^{3-}

Due to lack of data, the prediction methods presented above do not allow estimation of $\Delta H_{f,\text{el}}^\circ$ for V-apatites. Only two experimental $\Delta H_{f,\text{el}}^\circ$ for the synthetic vanadinite analog $\text{Pb}_{10}(\text{VO}_4)_6\text{Cl}_2$ are known. Therefore, an attempt was made to use the relationship between $\Delta H_{f,\text{el}}^\circ$ of apatite and $\Delta H_{f,\text{el}}^\circ$ of the AO_4^{3-} anion. The availability of experimental data allows to plot such a dependence only for lead apatites $\text{Pb}_{10}(\text{AO}_4)_6\text{Cl}_2$, where A=P, V, or As (Fig. 6). Since ideal linear fit is apparent ($R^2=1.00$), we hypothesize that linear correlation also exists for other apatite subgroups, with the same Me and X but different A. The lines drawn for the various P- and As-apatites (Fig. 7) allow to

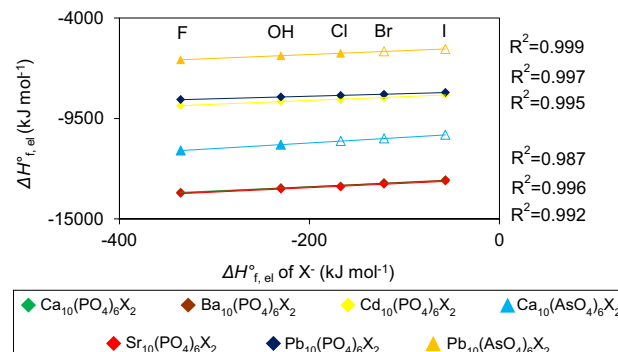


Fig. 5 Correlation of the $\Delta H_{f,\text{el}}^\circ$ of apatites vs. the $\Delta H_{f,\text{el}}^\circ$ of anions X^- . Experimental data and values predicted using Eq. 4 (Table 4) were used to plot regression lines (full symbols). Empty marks indicate values calculated from Eq. 5

Table 4 Comparison of the experimental enthalpies of formation with values predicted using U_{POT}

Apatite	exptl $\Delta H_{f,\text{el}}^\circ$ (kJ mol ⁻¹)	^a pred $\Delta H_{f,\text{el}}^\circ$ (kJ mol ⁻¹)	% diff
$\text{Ca}_{10}(\text{PO}_4)_6\text{F}_2$	-13,545	-13,546	-0.01
$\text{Ca}_{10}(\text{PO}_4)_6\text{Cl}_2$	-13,201	-13,196	0.04
$\text{Ca}_{10}(\text{PO}_4)_6\text{Br}_2$	-13,063	-13,067	-0.03
$\text{Ca}_{10}(\text{PO}_4)_6\text{I}_2$	-	-12,893	-
$\text{Sr}_{10}(\text{PO}_4)_6\text{F}_2$	-13,604	-13,604	0.00
$\text{Sr}_{10}(\text{PO}_4)_6\text{Cl}_2$	-13,233	-13,233	0.00
$\text{Sr}_{10}(\text{PO}_4)_6\text{Br}_2$	-	-13,111	-
$\text{Sr}_{10}(\text{PO}_4)_6\text{I}_2$	-	-12,926	-
$\text{Ba}_{10}(\text{PO}_4)_6\text{F}_2$	-13,564	-13,564	0.00
$\text{Ba}_{10}(\text{PO}_4)_6\text{Cl}_2$	-13,246	-13,246	0.00
$\text{Ba}_{10}(\text{PO}_4)_6\text{Br}_2$	-	-13,009	-
$\text{Ba}_{10}(\text{PO}_4)_6\text{I}_2$	-	-12,859	-
$\text{Cd}_{10}(\text{PO}_4)_6\text{F}_2$	-8795	-8795	0.00
$\text{Cd}_{10}(\text{PO}_4)_6\text{Cl}_2$	-8463	-8463	0.00
$\text{Cd}_{10}(\text{PO}_4)_6\text{Br}_2$	-	-8365	-
$\text{Cd}_{10}(\text{PO}_4)_6\text{I}_2$	-	-8199	-
$\text{Pb}_{10}(\text{PO}_4)_6\text{F}_2$	-8466	-8468	-0.02
$\text{Pb}_{10}(\text{PO}_4)_6\text{Cl}_2$	-8248	-8240	0.10
$\text{Pb}_{10}(\text{PO}_4)_6\text{Br}_2$	-8180	-8187	-0.08
$\text{Pb}_{10}(\text{PO}_4)_6\text{I}_2$	-	-8072	-

Note: exptl $\Delta H_{f,\text{el}}^\circ$ – experimental data extracted from Table 1; ^apred $\Delta H_{f,\text{el}}^\circ$ – calculated based on Eq. 4; %diff=100 · (exptl $\Delta H_{f,\text{el}}^\circ$ - ^apred $\Delta H_{f,\text{el}}^\circ$) / exptl $\Delta H_{f,\text{el}}^\circ$

Table 5 Comparison of the experimental enthalpies of formation and selected $\text{pred}\Delta H^\circ_{\text{f},\text{el}}$ from Table 4 with values predicted using $\Delta H^\circ_{\text{f},\text{el}}$ of monovalent anion X^-

Apatite	$\text{exptl}\Delta H^\circ_{\text{f},\text{el}}$ and $\text{pred}\Delta H^\circ_{\text{f},\text{el}}$ (kJ mol $^{-1}$)	$\text{pred}\Delta H^\circ_{\text{f},\text{el}}$ (kJ mol $^{-1}$)	% diff
$\text{Ca}_{10}(\text{PO}_4)_6\text{F}_2$	-13,545.0	-13,550.1	0.0
$\text{Ca}_{10}(\text{PO}_4)_6\text{OH}_2$	-13,292.0	-13,308.5	-0.1
$\text{Ca}_{10}(\text{PO}_4)_6\text{Cl}_2$	-13,200.8	-13,164.2	0.3
$\text{Ca}_{10}(\text{PO}_4)_6\text{Br}_2$	-13,063.0	-13,059.5	0.0
$\text{Ca}_{10}(\text{PO}_4)_6\text{I}_2$	-12,892.7	-12,911.4	-0.1
$\text{Sr}_{10}(\text{PO}_4)_6\text{F}_2$	-13,604.0	-13,618.7	-0.1
$\text{Sr}_{10}(\text{PO}_4)_6\text{OH}_2$	-13,373.0	-13,364.9	0.1
$\text{Sr}_{10}(\text{PO}_4)_6\text{Cl}_2$	-13,233.0	-13,213.3	0.1
$\text{Sr}_{10}(\text{PO}_4)_6\text{Br}_2$	-13,111.5	-13,103.2	0.1
$\text{Sr}_{10}(\text{PO}_4)_6\text{I}_2$	-12,926.3	-12,947.6	-0.2
$\text{Ba}_{10}(\text{PO}_4)_6\text{F}_2$	-13,564.0	-13,584.4	-0.2
$\text{Ba}_{10}(\text{PO}_4)_6\text{OH}_2$	-13,309.0	-13,318.3	-0.1
$\text{Ba}_{10}(\text{PO}_4)_6\text{Cl}_2$	-13,246.0	-13,159.4	0.7
$\text{Ba}_{10}(\text{PO}_4)_6\text{Br}_2$	-13,008.9	-13,044.0	-0.3
$\text{Ba}_{10}(\text{PO}_4)_6\text{I}_2$	-12,859.1	-12,880.9	-0.2
$\text{Cd}_{10}(\text{PO}_4)_6\text{F}_2$	-8795.0	-8797.7	0.0
$\text{Cd}_{10}(\text{PO}_4)_6\text{OH}_2$	-8565.8	-8577.6	-0.1
$\text{Cd}_{10}(\text{PO}_4)_6\text{Cl}_2$	-8463.0	-8446.1	0.2
$\text{Cd}_{10}(\text{PO}_4)_6\text{Br}_2$	-8365.2	-8350.7	0.2
$\text{Cd}_{10}(\text{PO}_4)_6\text{I}_2$	-8198.8	-8215.7	-0.2
$\text{Pb}_{10}(\text{PO}_4)_6\text{F}_2$	-8466.0	-8471.9	-0.1
$\text{Pb}_{10}(\text{PO}_4)_6\text{OH}_2$	-8325.2	-8325.0	0.0
$\text{Pb}_{10}(\text{PO}_4)_6\text{Cl}_2$	-8248.0	-8237.3	0.1
$\text{Pb}_{10}(\text{PO}_4)_6\text{Br}_2$	-8180.0	-8173.6	0.1
$\text{Pb}_{10}(\text{PO}_4)_6\text{I}_2$	-8072.1	-8083.6	-0.1
$\text{Ca}_{10}(\text{AsO}_4)_6\text{F}_2$	-11,258.8	-11,258.8	0.0
$\text{Ca}_{10}(\text{AsO}_4)_6\text{OH}_2$	-10,934.7	-10,934.7	0.0
$\text{Ca}_{10}(\text{AsO}_4)_6\text{Cl}_2$	-	-10,741.1	-
$\text{Ca}_{10}(\text{AsO}_4)_6\text{Br}_2$	-	-10,600.6	-
$\text{Ca}_{10}(\text{AsO}_4)_6\text{I}_2$	-	-10,401.9	-
$\text{Pb}_{10}(\text{AsO}_4)_6\text{F}_2$	-6288.0	-6286.8	0.0
$\text{Pb}_{10}(\text{AsO}_4)_6\text{OH}_2$	-6060.0	-6063.3	-0.1
$\text{Pb}_{10}(\text{AsO}_4)_6\text{Cl}_2$	-5931.8	-5929.8	0.0
$\text{Pb}_{10}(\text{AsO}_4)_6\text{Br}_2$	-	-5832.9	-
$\text{Pb}_{10}(\text{AsO}_4)_6\text{I}_2$	-	-5695.8	-

Note: $\text{exptl}\Delta H^\circ_{\text{f},\text{el}}$ – experimental data extracted from Table 1; $\text{pred}\Delta H^\circ_{\text{f},\text{el}}$ – calculated based on Eq. 4; $\text{pred}\Delta H^\circ_{\text{f},\text{el}}$ – calculated based on Eq. 5; %diff = 100 · ($\text{exptl}\Delta H^\circ_{\text{f},\text{el}} - \text{pred}\Delta H^\circ_{\text{f},\text{el}}$) / $\text{exptl}\Delta H^\circ_{\text{f},\text{el}}$ or %diff = 100 · ($\text{pred}\Delta H^\circ_{\text{f},\text{el}} - \text{exptl}\Delta H^\circ_{\text{f},\text{el}}$) / $\text{pred}\Delta H^\circ_{\text{f},\text{el}}$

determine the $\Delta H^\circ_{\text{f},\text{el}}$ of their vanadate counterparts. Linear regression coefficient a and b given in Table SI 7 were used to calculate $\text{pred}\Delta H^\circ_{\text{f},\text{el}}$ of V-apatites using Eq. 6:

$$\text{pred}\Delta H^\circ_{\text{f},\text{el}} = a \times \Delta H^\circ_{\text{f},\text{el}} \text{ of } \text{AO}_4^{3-} + b \quad (6)$$

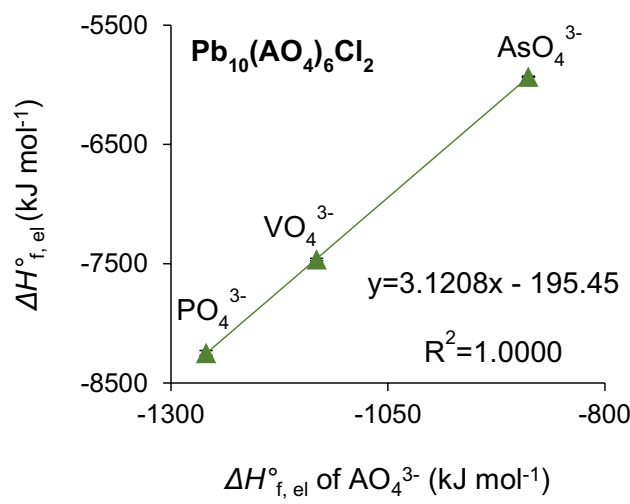


Fig. 6 Correlation of experimental $\Delta H^\circ_{\text{f},\text{el}}$ of Pb-apatites with $\Delta H^\circ_{\text{f},\text{el}}$ of tetrahedral anion AO_4^{3-} , where $\text{A}=\text{P}, \text{V}, \text{Cl}$

The $\Delta H^\circ_{\text{f},\text{el}}$ of AO_4^{3-} were extracted from Table SI 3. The results are summarized in Table 6. It is important to note that prediction of $\Delta H^\circ_{\text{f},\text{el}}$ for V-apatites would not have been possible without firstly estimating the values of $\Delta H^\circ_{\text{f},\text{el}}$ by the predictive methods described above.

Discussion

Experimental data selected from Table 1 and predicted values recommended in this work (Table 7) allow for comparison of $\Delta H^\circ_{\text{f},\text{el}}$ and presentation of the linear relationships observed within apatite subgroups (Fig. 8). The dependence of $\Delta H^\circ_{\text{f},\text{el}}$ on the molecular weight is apparent. The heavier halide substituted within any of the apatite subgroups the less negative $\Delta H^\circ_{\text{f},\text{el}}$ (apatite is less stable). This relationship is identical within all apatite subgroups studied but the intensity of this effect varies as evidenced by different slope coefficients of the trend lines. This observation also applies to the molecular weight of whole apatite. The lightest phosphate apatites have the most negative $\Delta H^\circ_{\text{f},\text{el}}$ and the heaviest lead arsenate apatites have the least negative $\Delta H^\circ_{\text{f},\text{el}}$. Therefore, $\text{Sr}_{10}(\text{PO}_4)_6\text{F}_2$ is enthalpically the most stable of all the apatites studied while $\text{Pb}_{10}(\text{AsO}_4)_6\text{I}_2$ is the least stable one.

The mass of the tetrahedral anion AO_4^{3-} and the mass of the anion at the X position strongly and equally affect the $\Delta H^\circ_{\text{f},\text{el}}$ but the mass of the metal cation Me^{2+} does not influence $\Delta H^\circ_{\text{f},\text{el}}$ unambiguously. Apatites containing alkaline earth metal cations ($\text{Ca}^{2+}, \text{Sr}^{2+}, \text{Ba}^{2+}$) are more enthalpically stable than apatites of other metals, e.g., Pb and Cd (but also Zn, Cu, Fe, see Drouet 2015, 2019), regardless of

Fig. 7 Plot of $\Delta H_{f,\text{el}}^\circ$ of apatites with $\Delta H_{f,\text{el}}^\circ$ of tetrahedral anion AO_4^{3-} for Pb- and Ca-apatites. Empty marks indicate values calculated from Eq. 6

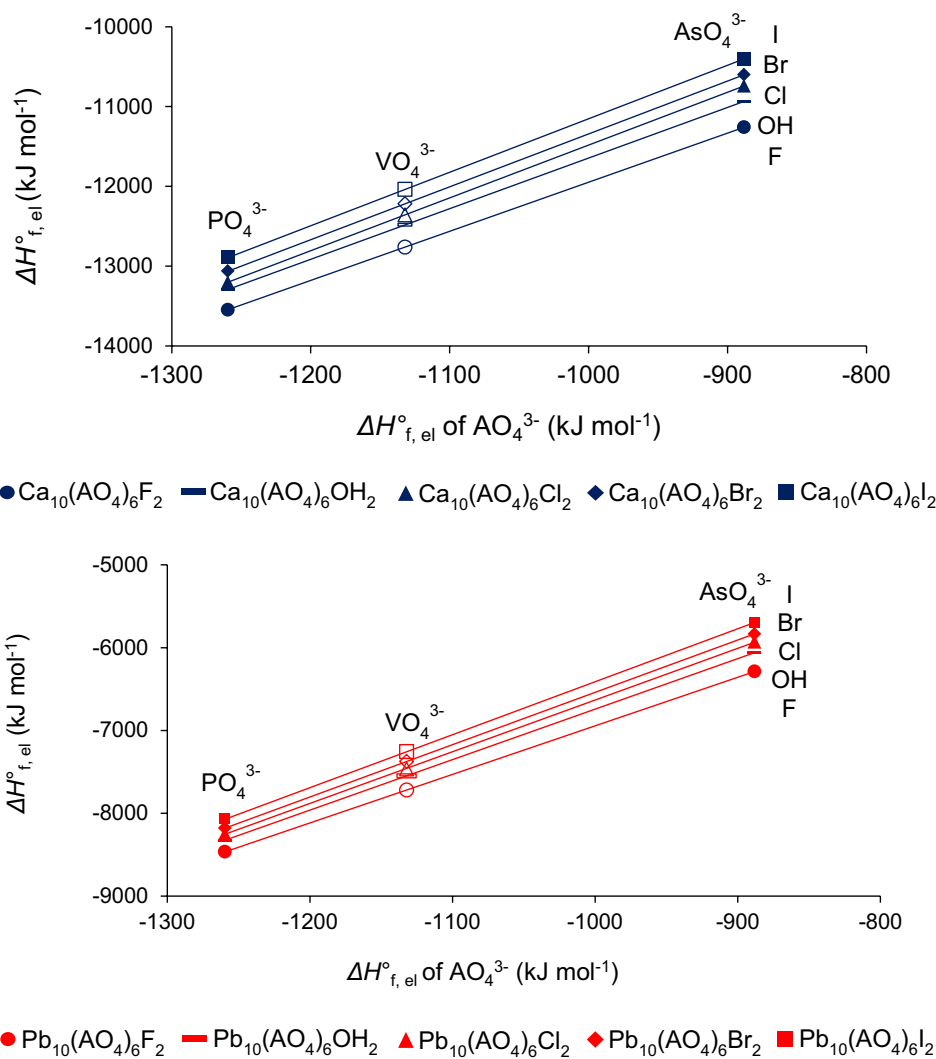


Table 6 Compilation of the experimental and predicted enthalpies of formation for phosphate, arsenate and vanadate Ca- and Pb-apatites

Apatite	$\text{exptl}\Delta H_{f,\text{el}}$ and ^a $\text{pred}\Delta H_{f,\text{el}}$ (kJ mol ⁻¹) A=P	$\text{exptl}\Delta H_{f,\text{el}}$ and ^b $\text{pred}\Delta H_{f,\text{el}}$ (kJ mol ⁻¹) A=As	$\text{exptl}\Delta H_{f,\text{el}}$ and ^c $\text{pred}\Delta H_{f,\text{el}}$ (kJ mol ⁻¹) A=V
$\text{Ca}_{10}(\text{AO}_4)_6\text{F}_2$	-13,545	-11,259	-12,761
$\text{Ca}_{10}(\text{AO}_4)_6\text{OH}_2$	-13,292	-10,935	-12,484
$\text{Ca}_{10}(\text{AO}_4)_6\text{Cl}_2$	-13,201	-10,741	-12,357
$\text{Ca}_{10}(\text{AO}_4)_6\text{Br}_2$	-13,063	-10,601	-12,218
$\text{Ca}_{10}(\text{AO}_4)_6\text{I}_2$	-12,893	-10,402	-12,038
$\text{Pb}_{10}(\text{AO}_4)_6\text{F}_2$	-8466	-6288	-7719
$\text{Pb}_{10}(\text{AO}_4)_6\text{OH}_2$	-8325	-6060	-7548
$\text{Pb}_{10}(\text{AO}_4)_6\text{Cl}_2$	-8248	-5932	-7465
$\text{Pb}_{10}(\text{AO}_4)_6\text{Br}_2$	-8180	-5833	-7375
$\text{Pb}_{10}(\text{AO}_4)_6\text{I}_2$	-8072	-5696	-7257

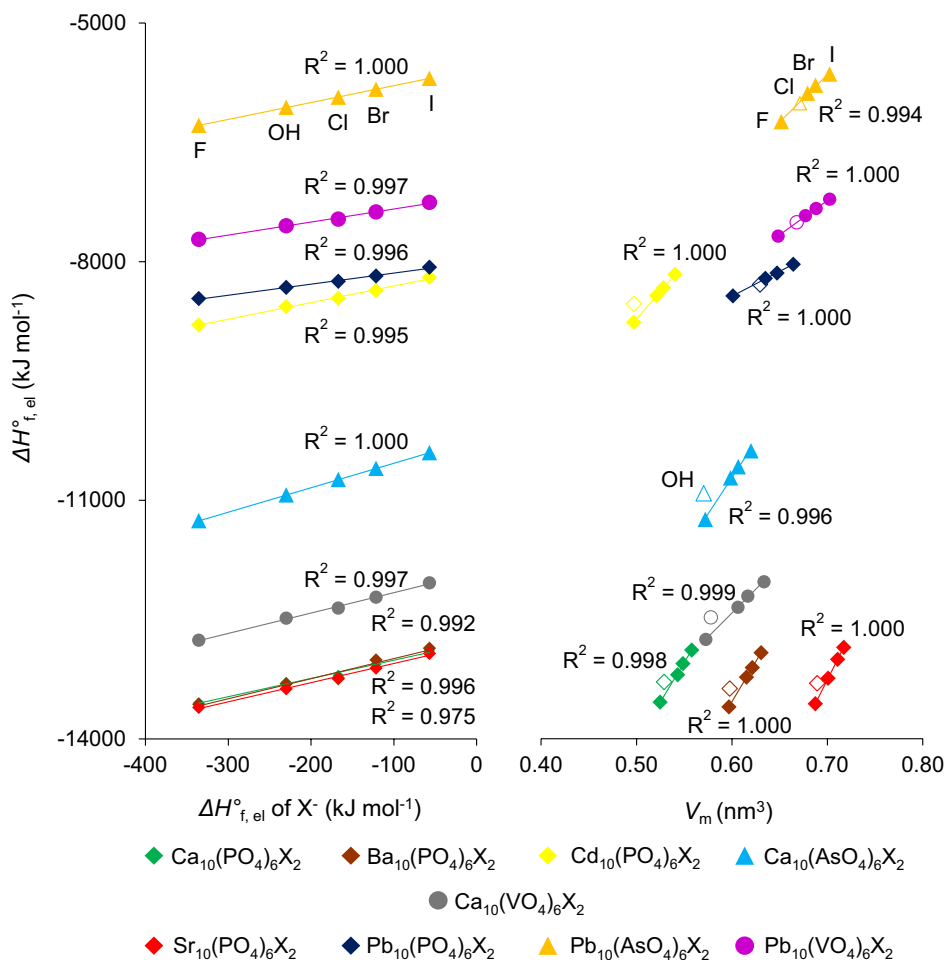
Note: $\text{exptl}\Delta H_{f,\text{el}}$ – experimental data extracted from Table 1; ^a $\text{pred}\Delta H_{f,\text{el}}$ – calculated based on Eq. 4; ^b $\text{pred}\Delta H_{f,\text{el}}$ – calculated based on Eq. 5; ^c $\text{pred}\Delta H_{f,\text{el}}$ – calculated based on Eq. 6

Table 7 Enthalpy of formation from elements $\Delta H_{f,el}^\circ$ for apatites recommended for use in thermodynamic calculations ($\text{recom}\Delta H_{f,el}^\circ$) in comparison with data obtained by two other prediction methods: ThermAP (Drouet 2015) and SSA (Glasser 2019)

Apatite	recom $\Delta H_{f,el}^\circ$ (kJ mol ⁻¹)	ThermAP $\Delta H_{f,el}^\circ$ (kJ mol ⁻¹)	% diff ¹	SSA $\Delta H_{f,el}^\circ$ (kJ mol ⁻¹)	% diff ²
Ca ₁₀ (PO ₄) ₆ F ₂	-13,545.0	-13,598.0	-0.39	-13,590.4	-0.34
Ca ₁₀ (PO ₄) ₆ OH ₂	-13,292.0	-13,373.0	-0.61	-13,348.5	-0.43
Ca ₁₀ (PO ₄) ₆ Cl ₂	-13,200.8	-13,258.0	-0.43	-13,157.8	0.33
Ca ₁₀ (PO ₄) ₆ Br ₂	-13,063.0	-12,833.0	1.76	-13,046.2	0.13
Ca ₁₀ (PO ₄) ₆ I ₂	-12,892.7	-	-	-12,895.9	-0.02
Sr ₁₀ (PO ₄) ₆ F ₂	-13,604.0	-13,604.0	0.00	-13,585.0	0.14
Sr ₁₀ (PO ₄) ₆ OH ₂	-13,373.0	-13,379.0	-0.04	-13,327.7	0.34
Sr ₁₀ (PO ₄) ₆ Cl ₂	-13,233.0	-13,265.0	-0.24	-13,197.6	0.27
Sr ₁₀ (PO ₄) ₆ Br ₂	-13,111.5	-12,839.0	2.08	-13,086.3	0.19
Sr ₁₀ (PO ₄) ₆ I ₂	-12,926.3	-	-	-12,926.8	0.00
Ba ₁₀ (PO ₄) ₆ F ₂	-13,564.0	-13,558.0	0.04	-13,483.1	0.60
Ba ₁₀ (PO ₄) ₆ OH ₂	-13,309.0	-13,333.0	-0.18	-13,220.7	0.66
Ba ₁₀ (PO ₄) ₆ Cl ₂	-13,246.0	-13,218.0	0.21	-13,135.2	0.84
Ba ₁₀ (PO ₄) ₆ Br ₂	-13,008.9	-12,793.0	1.66	-13,033.3	-0.19
Ba ₁₀ (PO ₄) ₆ I ₂	-12,859.1	-	-	-12,878.1	-0.15
Cd ₁₀ (PO ₄) ₆ F ₂	-8795.0	-8808.0	-0.15	-8686.4	1.23
Cd ₁₀ (PO ₄) ₆ OH ₂	-8565.8	-8583.0	-0.20	-8546.7	0.22
Cd ₁₀ (PO ₄) ₆ Cl ₂	-8463.0	-8469.0	-0.07	-8377.5	1.01
Cd ₁₀ (PO ₄) ₆ Br ₂	-8365.2	-8043.0	3.85	-8302.2	0.75
Cd ₁₀ (PO ₄) ₆ I ₂	-8198.8	-	-	-8189.0	0.12
Pb ₁₀ (PO ₄) ₆ F ₂	-8466.0	-8503.0	-0.44	-8944.9	-5.66
Pb ₁₀ (PO ₄) ₆ OH ₂	-8325.2	-8278.0	0.57	-8796.9	-5.67
Pb ₁₀ (PO ₄) ₆ Cl ₂	-8248.0	-8164.0	1.02	-8640.3	-4.76
Pb ₁₀ (PO ₄) ₆ Br ₂	-8180.0	-7738.0	5.40	-8559.6	-4.64
Pb ₁₀ (PO ₄) ₆ I ₂	-8072.1	-	-	-8456.4	-4.76
Ca ₁₀ (AsO ₄) ₆ F ₂	-11,258.8	-	-	-11,124.1	1.20
Ca ₁₀ (AsO ₄) ₆ OH ₂	-10,934.7	-	-	-10,882.2	0.48
Ca ₁₀ (AsO ₄) ₆ Cl ₂	-10,741.1	-	-	-10,691.5	0.46
Ca ₁₀ (AsO ₄) ₆ Br ₂	-10,600.6	-	-	-10,579.9	0.20
Ca ₁₀ (AsO ₄) ₆ I ₂	-10,401.9	-	-	-10,429.6	-0.27
Pb ₁₀ (AsO ₄) ₆ F ₂	-6288.0	-	-	-6004.6	4.51
Pb ₁₀ (AsO ₄) ₆ OH ₂	-6060.0	-	-	-5856.6	3.36
Pb ₁₀ (AsO ₄) ₆ Cl ₂	-5931.8	-	-	-5700.0	3.91
Pb ₁₀ (AsO ₄) ₆ Br ₂	-5832.9	-	-	-5619.3	3.66
Pb ₁₀ (AsO ₄) ₆ I ₂	-5695.8	-	-	-5516.1	3.16
Ca ₁₀ (VO ₄) ₆ F ₂	-12,761	-	-	-12,561.8	1.56
Ca ₁₀ (VO ₄) ₆ OH ₂	-12,484	-	-	-12,319.9	1.31
Ca ₁₀ (VO ₄) ₆ Cl ₂	-12,357	-	-	-12,129.2	1.84
Ca ₁₀ (VO ₄) ₆ Br ₂	-12,218	-	-	-12,017.6	1.64
Ca ₁₀ (VO ₄) ₆ I ₂	-12,038	-	-	-11,867.3	1.42
Pb ₁₀ (VO ₄) ₆ F ₂	-7719	-	-	-	-
Pb ₁₀ (VO ₄) ₆ OH ₂	-7548	-	-	-	-
Pb ₁₀ (VO ₄) ₆ Cl ₂	-7465	-	-	-	-
Pb ₁₀ (VO ₄) ₆ Br ₂	-7375	-	-	-	-
Pb ₁₀ (VO ₄) ₆ I ₂	-7257	-	-	-	-

Note: bold – experimental data extracted from Tab. 1; *italics* – values predicted in this work; %diff¹ = 100 · (ThermAP $\Delta H_{f,el}^\circ$ —recom $\Delta H_{f,el}^\circ$) / recom $\Delta H_{f,el}^\circ$; %diff² = 100 · (SSA $\Delta H_{f,el}^\circ$ —recom $\Delta H_{f,el}^\circ$) / recom $\Delta H_{f,el}^\circ$

Fig. 8 Linear relationships between recommended $\Delta H_{f,\text{el}}^\circ$ (Table 8) and $\Delta H_{f,\text{el}}^\circ$ of X^- and V_m seen within apatite subgroups. Empty marks indicate values for OH-apatites not included in regression. Error bars from literature where available



substitution at the A or X position. However, the difference between $\Delta H_{f,\text{el}}^\circ$ of phosphate apatites containing Ca^{2+} , Sr^{2+} or Ba^{2+} is minimal compared to the differences with other apatites (even though the difference in the molecular mass of these cations is very pronounced, and the contribution of the cation to the formula is the largest). This may indicate that it is the chemical character of the Me^{2+} bond in the apatite structure that has also a strong effect on the $\Delta H_{f,\text{el}}^\circ$. The chemical character of the bonds is similar within alkali earth elements (Ca^{2+} , Sr^{2+} , and Ba^{2+}) and different for heavy metals (Pb^{2+} , Cd^{2+} , etc.).

Hydroxylapatites fit well into linear regression line in the relationship between $\Delta H_{f,\text{el}}^\circ$ of apatite and $\Delta H_{f,\text{el}}^\circ$ of X^- (Fig. 8A). This is somewhat obvious since the enthalpy of X^- is the component for the calculation of the enthalpy of apatite formation. Such complete linear dependencies are rare. Deviations of hydroxylapatites from the trend line are more often observed as in the case of $\Delta H_{f,\text{el}}^\circ$ of apatite versus V_m (Fig. 8B). This reflects the dissimilarity of the OH^- anion from the halide anion, due, among other things, to the anisotropy of the charge distribution. The presence of such an anion in the hexagonal tunnel of the apatite

crystalline structure imposes a higher energy penalty resulting in higher $\Delta H_{f,\text{el}}^\circ$ (more endothermic). The presence of H^+ on the OH^- group can also lead to hydrogen bonding effects within apatite channels, probably causing a stabilizing effect. Additionally, the OH^- ions in the X-position ions in the channels within the apatite structure do not occupy the same positions in the z value along the *c*-axis. A larger X-site anion results in more separation from the mirror plane of the triangular cationic II sites.

The recommended $\Delta H_{f,\text{el}}^\circ$ (Table 8) show linear correlation also with the electronegativity of the halide X, the ionization energy of the halide X and the $\Delta H_{f,\text{el}}^\circ$ of MeX_2 (Figs. SI 1, 2, 3). All relationships give a very good or good linear fit. These correlations have been reported before but referred only to experimental data (Cruz et al. 2005b; Drouet 2015; Puzio et al. 2022). The fact that the experimental and predicted values match these lines equally well can be taken as evidence of their reliability.

Linear relationships between selected parameters within apatite subgroups are used to predict missing thermodynamic data by regression analysis. The proposed complete procedure consists of 5 steps and is shown in Table 9. The

Table 8 The prediction method for standard enthalpies of apatites using the molar volume, lattice energy, $\Delta H_{f,el}^\circ$ of anions AO_4^{3-} or X^- and linear regression

Step	Procedure
1	Compilation of existing experimental molar volume V_m data for apatites and estimation of missing data (where possible) based on the linear relationship of V_m with halide ionic radius $R_i(\text{X}^-)$ plotted separately for the halide apatite subgroups
2	Compilation of existing lattice energy U_{POT} experimental data and estimation of missing data (where possible) based on the linear dependence of U_{POT} on V_m plotted separately for the halide apatite subgroups (utilizing both experimental V_m and values predicted in step 1)
3	Compilation of existing experimental enthalpies of formation from elements $\Delta H_{f,el}^\circ$ for apatites and estimation of the missing data (where possible) based on linear relationship of $\Delta H_{f,el}^\circ$ of apatites with U_{POT} plotted separately for the halide apatite subgroups
4	Using the experimental $\Delta H_{f,el}^\circ$ and values predicted for apatites in step 3, estimation of missing values (where possible) from the linear relationship of $\Delta H_{f,el}^\circ$ of apatites with $\Delta H_{f,el}^\circ$ of halide anions X^- plotted separately for the halide subgroups
5	Using the experimental $\Delta H_{f,el}^\circ$ and values predicted in the steps above, estimation of missing values (where possible) based on the linear relationship of $\Delta H_{f,el}^\circ$ of apatites with $\Delta H_{f,el}^\circ$ of tetrahedral anions AO_4^{3-} plotted separately for the apatite subgroups containing the same Me^{2+} cations and the same X^- anions

order in which the calculations are performed is crucial because only by supplementing the database with the values obtained from one prediction could the calculations for obtaining subsequent prediction values be performed. This procedure allowed for the prediction of 22 thus far experimentally unknown $\Delta H_{f,el}^\circ$ values for apatite end-members. This includes 9 values for iodoapatites which are the least characterized apatites. The percentage relative difference which is a measure of precision is in most cases less than 1%. The prediction precision is due to the high regression coefficients (above $R^2=0.98$). Such precision is comparable to the experimental uncertainty obtained when reproducing experimental data using calorimetric measurements or dissolution experiments. It is also higher than in other prediction methods proposed so far.

Using the $\Delta H_{f,el}^\circ$ recommended in this work the solubility constants $K_{\text{sp},298.15\text{K}}$ can be calculated and compared where available with experimental data. It is based on dissolution reaction:



$\text{Log}K_{\text{sp},298.15\text{K}}$ is calculated from the equation:

$$\log K_{\text{sp},298.15\text{K}} = \log e^{\frac{-\Delta G_f^\circ}{RT}} \quad (8)$$

where ΔG_f° is the free Gibbs energy of the dissolution reaction (7), T is temperature (in K), R is the gas constant ($8.31447 \text{ J mol}^{-1}\text{K}^{-1}$) and superscript “°” denotes normal conditions. The thermodynamic data used in calculations are provided in Tables SI 3 and SI 9. Comparison of the calculated $K_{\text{sp},298.15\text{K}}$ with previously reported values indicates very good or good agreement within the experimental error (Tab. SI 9). This confirms the usefulness and reliability of the $\Delta H_{f,el}^\circ$ predicted here for thermodynamic calculations.

Conclusions

A method for predicting the $\Delta H_{f,el}^\circ$ of apatites using molar volume, lattice energy, and $\Delta H_{f,el}^\circ$ of anions AO_4^{3-} or X^- was proposed and demonstrated on phosphate, arsenate, and vanadate apatites containing Ca, Sr, Ba, Pb, and Cd at the cationic positions and F, OH, Cl, Br, and I at the halide position. The approach is based on regression analysis of the correlations occurring within apatite subgroups. These subgroups are formed by $\text{Me}_{10}(\text{AO}_4)_6\text{X}_2$ apatites with the same Me^{2+} cations and tetrahedral AO_4^{3-} anions and with different halides in the X position (or a complex monovalent OH^- anion). This approach not only leads to more accurate predictions (with precision comparable with the experimental uncertainty) but allows to see important relationships between apatites and should also be used when analyzing other properties of apatite end-members. The proposed prediction procedure allowed for the prediction of 22 so far unknown $\Delta H_{f,el}^\circ$ and can be applied to a wider range of apatites than other methods. Due to lack of experimental data, it is still not possible to predict the $\Delta H_{f,el}^\circ$ for $\text{Sr}_{10}(\text{VO}_4)_6\text{X}_2$, $\text{Ba}_{10}(\text{VO}_4)_6\text{X}_2$, $\text{Cd}_{10}(\text{AsO}_4)_6\text{X}_2$, $\text{Sr}_{10}(\text{AsO}_4)_6\text{X}_2$ or $\text{Ba}_{10}(\text{AsO}_4)_6\text{X}_2$. The new prediction method for $\Delta H_{f,el}^\circ$ of apatites could provide important insights, e.g., allowing optimization of the chemical composition and properties of apatite-based materials for their suitability to various forms of nuclear waste deposited in geological repositories.

Supplementary Information The online version contains supplementary material available at <https://doi.org/10.1007/s00410-022-01964-z>.

Acknowledgements The authors would like to thank the two anonymous reviewers for their diligent and very thorough work on the manuscript.

Authors contributions Conceptualization; Methodology; Formal analysis; Investigation resources; Data curation; Writing—original draft

preparation; Visualization; Project administration; Funding acquisition: Bartosz Puzio; Writing—review and editing; supervision: Maciej Manecki. All authors have read and agreed to the published version of the manuscript.

Funding The authors have no relevant financial or non-financial interests to disclose. The research leading to these results received funding from the Polish National Science Center (NCN) under Grant Agreement [Grant No. 2017/27/N/ST10/00776].

Open Access This article is licensed under a Creative Commons Attribution 4.0 International License, which permits use, sharing, adaptation, distribution and reproduction in any medium or format, as long as you give appropriate credit to the original author(s) and the source, provide a link to the Creative Commons licence, and indicate if changes were made. The images or other third party material in this article are included in the article's Creative Commons licence, unless indicated otherwise in a credit line to the material. If material is not included in the article's Creative Commons licence and your intended use is not permitted by statutory regulation or exceeds the permitted use, you will need to obtain permission directly from the copyright holder. To view a copy of this licence, visit <http://creativecommons.org/licenses/by/4.0/>.

References

- Aissa A, Badraoui B, Thouvenot R, Debbabi M (2004) (2004) Synthesis, x-ray structural analysis and spectroscopic investigations (IR and 31P MAS NMR) of mixed barium/strontium fluoroapatites. *Eur J Inorg Chem* 19:3828–3836. <https://doi.org/10.1002/ejic.200400224>
- Alberius HP, Lidin S, Petříček V (1999) Iodo-oxyapatite, the first example from a new class of modulated apatites. *Acta Crystall B-Stru* 55(2):165–169. <https://doi.org/10.1107/S0108768198012312>
- Alberius-Henning P, Mattsson C, Lidin S (2000) Crystal structure of pentastrontium tris (phosphate) bromide, $\text{Sr}_5(\text{PO}_4)_3\text{Br}$ and of pentabarium tris (phosphate) bromide $\text{Ba}_5(\text{PO}_4)_3\text{Br}$, two bro-moapatites. *Z Krist-New Crys St* 215(3):345–346. <https://doi.org/10.1515/ncts-2000-0319>
- Allison JD, Brown DS, Novo-Gradac KJ (1991) MINTEQA2/PRODEFA2, a geochemical assessment model for environmental systems: version 3.0 user's manual. Environmental Research Laboratory, Office of Research and Development, US Environmental Protection Agency, Athens, Georgia
- Amjad Z, Koutsoukos PG, Nancollas GH (1981) The mineralization of enamel surfaces. A constant composition kinetics study. *J Dent Res* 60(10):1783–1792. <https://doi.org/10.1177/00220345810600100901>
- Antao SM, Dhaliwal I (2018) Lead apatites: structural variations among $\text{Pb}_5(\text{BO}_4)_3\text{Cl}$ with B=P (pyromorphite), As (mimetite) and V (vanadinite). *J Synchrotron Radiat* 25(1):214–221. <https://doi.org/10.1107/S1600577517014217>
- Audubert F, Savariault JM, Lacout JL (1999) Pentalead tris (vanadate) iodide, a defect vanadinite-type compound. *Acta Crystall c* 55(3):271–273. <https://doi.org/10.1107/S0108270198005034>
- Avnimelech Y, Moreno EC, Brown WE (1973) Solubility and surface properties of finely divided hydroxyapatite. *J Res NBS a Phys Ch* 77(1):149. <https://doi.org/10.6028/jres.077A.008>
- Babu R, Jena H, Kutty KG, Nagarajan K (2011) Thermodynamic functions of $\text{Ba}_{10}(\text{PO}_4)_6\text{Cl}_2$, $\text{Sr}_{10}(\text{PO}_4)_6\text{Cl}_2$ and $\text{Ca}_{10}(\text{PO}_4)_6\text{Cl}_2$. *Thermochim Acta* 526(1–2):78–82. <https://doi.org/10.1016/j.tca.2011.08.027>
- Baikie T, Mercier PH, Elcombe MM, Kim JY, Le Page Y, Mitchell LD, White TJ, Whitfield PS (2007) Triclinic apatites. *Acta Crystall B-Stru* 63(2):251–256. <https://doi.org/10.1107/S0108768106053316>
- Bajda T, Szmith E, Manecki M (2007) Removal of As(V) from solutions by precipitation of mimetite $\text{Pb}_5(\text{AsO}_4)_3\text{Cl}$. *Environ. Engn.* 1:119–124
- Bajda T (2010) Solubility of mimetite $\text{Pb}_5(\text{AsO}_4)_3\text{Cl}$ at 5–55 °C. *Environ Chem* 7:268–278. <https://doi.org/10.1071/EN10021>
- Baker WE (1966) An X-ray diffraction study of synthetic members of the pyromorphite series. *Am Mineral J Earth Planet Mater* 51(11–12):1712–1721
- Ball JW, Nordstrom DK, Jenne EA (1980) Additional and revised thermochemical data and computer code for WATEQ2: A computerized chemical model for trace and major element speciation and mineral equilibria of natural waters (Vol. 78). US Geological Survey, Menlo Park, California
- Baran EJ (1972) Kristallographische Daten einiger Vanadin-Bromapatite. *Monatsh Chem* 103(6):1684–1690. <https://doi.org/10.1007/BF00904623>
- Beck HP, Douihéche M, Haberkorn R, Kohlmann H (2006) Synthesis and characterisation of chloro-vanadato-apatites $\text{M}_5(\text{VO}_4)_3\text{Cl}$ ($\text{M}=\text{Ca}, \text{Sr}, \text{Ba}$). *Solid State Sci* 8(1):64–70. <https://doi.org/10.1016/j.solidstatesciences.2005.08.014>
- Bell LC, Mika H, Kruger BJ (1978) Synthetic hydroxyapatite-solubility product and stoichiometry of dissolution. *Arch Oral Biol* 23(5):329–336. [https://doi.org/10.1016/0003-9969\(78\)90089-4](https://doi.org/10.1016/0003-9969(78)90089-4)
- Bell AM, Henderson CMB, Wendlandt RF, Harrison WJ (2008) Rietveld refinement of $\text{Ba}_5(\text{AsO}_4)_3\text{Cl}$ from high-resolution synchrotron data. *Acta Crystallogr e* 64(9):i63–i64. <https://doi.org/10.1107/S1600536808026901>
- Bell AM, Henderson CMB, Wendlandt RF, Harrison WJ (2009) Rietveld refinement of $\text{Sr}_5(\text{AsO}_4)_3\text{Cl}$ from high-resolution synchrotron data. *Acta Crystallogr e* 65(3):i16–i17. <https://doi.org/10.1107/S1600536809005054>
- Ben Cherifa A, Nounah A, Lacout JL, Jemal M (2001) Synthèse et thermochimie de phosphates au cadmium. *Thermochimica Acta* 366(1):7–13. [https://doi.org/10.1016/S0040-6031\(00\)00713-9](https://doi.org/10.1016/S0040-6031(00)00713-9)
- Bhatnagar VM (1970) Preparation, lattice parameters and X-ray powder patterns of lead fluorapatite and lead chlorapatite. *Inorg Nucl Chem Lett* 6(12):913–917. [https://doi.org/10.1016/0020-1650\(70\)80074-5](https://doi.org/10.1016/0020-1650(70)80074-5)
- Biagioni C, Pasero M (2013) The crystal structure of johnbaumite, $\text{Ca}_5(\text{AsO}_4)_3\text{OH}$, the arsenate analogue of hydroxylapatite. *Am Mineral* 98(8–9):1580–1584. <https://doi.org/10.2138/am.2013.4443>
- Biagioni C, Bosi F, Hålenius U, Pasero M (2017) The crystal structure of turneaureite, $\text{Ca}_5(\text{AsO}_4)_3\text{Cl}$, the arsenate analog of chlorapatite, and its relationships with the arsenate apatites johnbaumite and svabite. *Am Mineral* 102(10):1981–1986. <https://doi.org/10.2138/am-2017-6041>
- Bigi A, Foresti E, Marchetti F, Ripamonti A, Roveri N (1984) Barium calcium hydroxyapatite solid solutions. *J Chem Soc Dalton* 6:1091–1093. <https://doi.org/10.1039/DT9840001091>
- Bisengalieva MR, Ogorodova LP, Vigasina MF, Melchakova LV (2010) Calorimetric determination enthalpy of the formation of natural pyromorphite. *Russ J Phys Chem A* 84:1838–1840. <https://doi.org/10.1134/S0036024410110038>
- Bogach VV, Dobrydnev SV, Beskov VS (2001) Calculation of the thermodynamic properties of apatites. *Russ J Inorg Chem* 46(7):1011–1014
- Bondareva OS, Malinovskii YA (1986) Crystal structure of synthetic Ba hydroxyapatite. *Kristallografiya* 31(2):233–236
- Bothe JV Jr, Brown PW (1999) The stabilities of calcium arsenates at 23 ± 1 °C. *J Hazard Mater* 69(2):197–207. [https://doi.org/10.1016/S0304-3894\(99\)00105-3](https://doi.org/10.1016/S0304-3894(99)00105-3)

- Brenner P, Engel G, Wondratschek H (1970) Blei-Apatite mit Überstruktur. *Z Krist-Cryst Mater* 131(1–6):206–212. <https://doi.org/10.1524/zkri.1970.131.16.206>
- Bulanov EN, Petrov SS, Xu Z, Knyazev AV, Skoblikov NE (2021) Synthesis and crystal structure of some Ba-apatites. *Russ J Inorg Chem* 66(4):455–459. <https://doi.org/10.1134/S0036023621040069>
- Calos NJ, Kennard CH, Davis RL (1990) Crystal structure of mimetite, $Pb_5(AsO_4)_3Cl$. *Z Kristallogr* 191(1–2):125–129. <https://doi.org/10.1524/zkri.1990.191.1-2.125>
- Cao C, Chong S, Thirion L, Mauro JC, McCloy JS, Goel A (2017) Wet chemical synthesis of apatite-based waste forms—A novel room temperature method for the immobilization of radioactive iodine. *J Mater Chem a* 5(27):14331–14342. <https://doi.org/10.1039/C7TA00230K>
- Chai BH (2020) Optical crystals. In CRC handbook of laser science and technology (pp. 3–65). CRC Press
- Chance MW (2014) Hydroflux synthesis: a new and effective technique for exploratory crystal growth
- Cherifa AB, Khattech I, Jemal M (1988) A fast and direct method for the preparation of hydroxyapatite. *Chem. Inform.* 19(24):1
- Cherifa AB, Somrani S, Jemal M (1991) Détermination de l'enthalpie standard de formation de la fluorapatite de l'hydroxyapatite et de la chlorapatite. *J Chim Phys* 88: 1893–1900 (in French). <https://doi.org/10.1051/jcp/1991881893>
- Cherifa AB, Jemal M (2004) Enthalpy of formation and mixing of calcium-cadmium phosphoapatites. *Phosph Res Bull* 15:113–118. https://doi.org/10.3363/prb1992.15.0_113
- Chermak JA, Rimstidt JD (1989) Estimating the thermodynamic properties (ΔG°_f and ΔH°_f) of silicate minerals at 298 K from the sum of polyhedral contributions. *Am Miner* 74(9–10):1023–1031
- Chernorukov NG, Knyazev AV, Bulanov EN (2010) Isomorphism and phase diagram of the $Pb_5(PO_4)_3Cl$ - $Pb_5(VO_4)_3Cl$ system. *Russ J Inorg Chem* 55(9):1463–1470. <https://doi.org/10.1134/S0036023610090226>
- Chernorukov NG, Knyazev AV, Bulanov EN (2011) Phase transitions and thermal expansion of apatite-structured compounds. *Inorg Mater* 47(2):172–177. <https://doi.org/10.1134/S002016851101002X>
- Chin KA, Nancollas GH (1991) Dissolution of fluorapatite. A constant-composition kinetics study. *Langmuir* 7(10):2175–2179
- Corker DL, Chai BH, Nicholls JOHN, Loutts GB (1995) Neodymium-doped $Sr_5(PO_4)_3F$ and $Sr_5(VO_4)_3F$. *Acta Crystallogr C* 51(4):549–551. <https://doi.org/10.1107/S0108270194006906>
- Coulon A, Laurencin D, Grandjean A, Le Gallet S, Minier L, Rossignol S, Campayo L (2016) Key parameters for spark plasma sintering of wet-precipitated iodate-substituted hydroxyapatite. *J Eur Ceram Soc* 36(8):2009–2016. <https://doi.org/10.1016/j.jeurceramsoc.2016.02.041>
- Coulon A, Grandjean A, Laurencin D, Jollivet P, Rossignol S, Campayo L (2017) Durability testing of an iodate-substituted hydroxyapatite designed for the conditioning of 129I. *J Nucl Mater* 484:324–331. <https://doi.org/10.1016/j.jnucmat.2016.10.047>
- Craig RG, Rootare HM (1974) Heats of solution of apatites, human enamel and dicalcium-phosphate in dilute hydrochloric acid. In Analytical Calorimetry (pp. 397–405). Springer, Boston, MA
- Cruz FJ, Canongia Lopes JN, Calado JC, Minas da Piedade ME (2005a) A molecular dynamics study of the thermodynamic properties of calcium apatites 1. Hexagonal phases. *J Phys Chem B* 99(51):24473–24479. <https://doi.org/10.1021/jp054304p>
- Cruz FJAL, da Piedade MEM, Calado JCG (2005b) Standard molar enthalpies of formation of hydroxy-, chlor-, and bromapatite. *J Chem Therm* 37:1061–1070. <https://doi.org/10.1016/j.jct.2005.01.010>
- Dachs E, Harlov D, Benisek A (2010) Excess heat capacity and entropy of mixing along the chlorapatite–fluorapatite binary join. *Phys Chem Miner* 37(9):665–676. <https://doi.org/10.1007/s00269-010-0366-3>
- Dai Y, Hughes JM (1989) Crystal structure refinements of vanadinite and pyromorphite. *Can Mineral* 27(2):189–192
- Dai Y, Hughes JM, Moore PB (1991) The crystal of mimetite and clinomimetite, $Pb_5(AsO_4)_3Cl$. *Can Mineral* 29(2):369–376
- Davis RJ (1973) (P.) Eckerlin and (H.) Kandler. Landolt-Börnstein. Numerical data and functional relationships in science and technology New Series. Group III: Crystal and solid state physics. Volume 6. Structure data of elements and intermetallic phases. Berlin, Heidelberg, and New York (Springer-Yerlag), xxviii+ 1019 pp 1971. Price DM 620.00 (\$179.10). *Mineral Mag* 39(301): 127–128. <https://doi.org/10.1017/minmag.1973.039.301.27>
- Dong ZL, White TJ (2004) Calcium–lead fluoro-vanadinite apatites I Disequilibrium Structures. *Acta Crystall B-Stru* 60(2):138–145. <https://doi.org/10.1107/S0108768104001831>
- Dorđević T, Šutović S, Stojanović J, Karanović L (2008) Sr, Ba and Cd arsenates with the apatite-type structure. *Acta Crystall c* 64(9):182–186. <https://doi.org/10.1107/S0108270108023457>
- Driessens FCM, Verbeeck RMH (1982) The probable phase composition of the mineral in sound enamel and dentine. *Bull Soc Chim Bel* 91(7):573–596. <https://doi.org/10.1002/bscb.19820910702>
- Drouet C (2015) A comprehensive guide to experimental and predicted thermodynamic properties of phosphate apatite minerals in view of applicative purposes. *J Chem Therm* 81:143–159. <https://doi.org/10.1016/j.jct.2014.09.012>
- Drouet C (2019) Applied predictive thermodynamics (ThermAP). Part 2. Apatites containing Ni^{2+} , Co^{2+} , Mn^{2+} , or Fe^{2+} ions. *J Chem Therm* 136:182–189. <https://doi.org/10.1016/j.jct.2015.06.016>
- Duan CJ, Wu XY, Liu W, Chen HH, Yang XX, Zhao JT (2005) X-ray excited luminescent properties of apatitic compounds $Ba_5(PO_4)_3X$ (X : OH^- , Cl^- , Br^-): structure and hydroxyl ion conductivity of barium hydroxyapatite. *J Alloy Compd* 396(1–2):86–91. <https://doi.org/10.1016/j.jallcom.2004.11.064>
- Dunn PJ, Rouse RC (1978) Morelandite, a new barium arsenate chloride member of the apatite group. *Can Mineral* 16(4):601–604
- Dunn PJ, Peacor DR, Newberry N (1980) Johnbaumite, a new member of the apatite group from Franklin, New Jersey. *Am Mineral* 65(11–12):1143–1145
- Dunn PJ, Petersen EU, Peacor DR (1985) Turneaureite, a new member of the apatite group from Franklin, New Jersey, Balmat, New York and Långban, Sweden. *Can Mineral* 23(2):251–254
- Dykes E (1974) Preparation and characterisation of calcium bromapatite. *Mater Res Bull* 9(9):1227–1236. [https://doi.org/10.1016/0025-5408\(74\)90041-5](https://doi.org/10.1016/0025-5408(74)90041-5)
- Dziura A, Kwaśniak-Kominek M, Manecki M, Bajda T (2012) Low temperature synthesis and thermodynamic stability of fluoropyromorphite $Pb_5(PO_4)_3F$ at 5–65 °C. *Geol Geophys Environ* 38(4):465
- Egan EP Jr, Wakefield ZT, Elmore KL (1950) High-temperature heat content of hydroxyapatite. *J Am Chem Soc* 72(6):2418–2421
- Egan EP Jr, Wakefield ZT, Elmore KL (1951) Low-Temperature Heat Capacity and Entropy of Hydroxyapatite I. *J Am Chem Soc* 73(12):5579–5580
- El Feki H, Amami M, Ben SA, Jemal M (2004) Synthesis of potassium chloroapatites, IR, X-ray and Raman studies. *Phys Status Solidi C* 1(7):1985–1988. <https://doi.org/10.1002/pssc.200304450>
- Elasri S, Cherifa AB, Bouhaouss A, Ferhat M, Jemal M (1995) Mécanisme de dissolution du phosphate tricalcique β et de l'hydroxyapatite dans l'acide phosphorique. *Thermochim Acta* 249:121–126. [https://doi.org/10.1016/0040-6031\(95\)90680-0](https://doi.org/10.1016/0040-6031(95)90680-0)
- Elliott JC, Dykes E, Mackie PE (1981) Structure of bromapatite and the radius of the bromide ion. *Acta Crystall B-Stru* 37(2):435–438. <https://doi.org/10.1107/S0567740881003208>

- Elliott JC (1994) Hydroxyapatites and nonstoichiometric apatites. *Stud Inorg Chem* 18:111–189
- Engel G (1970) Hydrothermalsynthese von bleihydroxylapatiten $Pb_5(XO_4)_3OH$ mit $X = P$, As, V. *Naturwissenschaften*. 57(7): 355–355. <https://doi.org/10.1007/BF01173112>
- Farr TD, Elmore KL (1962) System $CaO-P_2O_5-HF-H_2O$: thermodynamic properties. *J Phys Chem* 66:315–318
- Fleche JL (2002) Thermodynamical functions for crystals with large unit cells such as zircon, coffinite, fluorapatite, and iodoapatite from ab initio calculations. *Phys Rev B* 65(24):245116. <https://doi.org/10.1103/PhysRevB.65.245116>
- Flis J, Borkiewicz O, Bajda T, Manecki M, Klasa J (2010) Synchrotron-based X-ray diffraction of the lead apatite series $Pb_{10}(PO_4)_6Cl_2-Pb_{10}(AsO_4)_6Cl_2$. *J Synchrotron Radiat* 17(2):207–214. <https://doi.org/10.1107/S0909049509048705>
- Flis J, Manecki M, Bajda T (2011) Solubility of pyromorphite $Pb_5(PO_4)_3Cl$ -mimetic $Pb_5(AsO_4)_3Cl$ solid solution series. *Geochim Cosmochim Ac* 75(7):1858–1868. <https://doi.org/10.1016/j.gca.2011.01.021>
- Flora NJ, Hamilton KW, Schaeffer RW, Yoder CH (2004a) A comparative study of the synthesis of calcium, strontium, barium, cadmium, and lead apatites in aqueous solution. *Syn React Inorg Met* 34(3):503–521. <https://doi.org/10.1081/SIM-120030437>
- Flora NJ, Yoder CH, Jenkins HDB (2004b) Lattice energies of apatites and the estimation of $\Delta H_f^\circ(PO_4^{3-}, g)$. *Inorg Chem* 43(7):2340–2345. <https://doi.org/10.1021/ic030255o>
- Gerke TL, Scheckel KG, Schock MR (2009) Identification and distribution of vanadinite ($Pb_5(V^{5+}O_4)_3Cl$) in lead pipe corrosion by-products. *Environ Sci Technol* 43(12):4412–4418. <https://doi.org/10.1021/es900501t>
- Getman YI, Ardanova LL, Marchenko VI, Grigoreva AA, Vasilenko TA, Ulyanova YV (2001) Substitution of calcium by sodium with neodymium, samarium, gadolinium, and holmium in vanadium hydroxyapatite. *Ukr Khim Zh* 67(1–2):16–19
- Getman EI, Marchenko VI, Loboda SN, Yablochkova NV, Plehov AL (2007) Isomorphic substitution of samarium for strontium in the $Sr_5(VO_4)_3OH$ structure. *Aip Conf Proc* 14(3):317–320
- Glasser L (2019) Apatite Thermochemistry: The Simple Salt Approximation. *Inorg Chem* 58(19):13457–13463. <https://doi.org/10.1021/acs.inorgchem.9b02343>
- Glasser L, Jenkins HDB (2000) Lattice energies and unit cell volumes of complex ionic solids. *J Am Chem Soc* 122(4):632–638. <https://doi.org/10.1021/ja992375u>
- Glasser L, Jenkins HDB (2008) Internally consistent ion volumes and their application in volume-based thermodynamics. *Inorg Chem* 47(14):6195–6202. <https://doi.org/10.1021/ic702399u>
- Glasser L, Jenkins HDB (2009) Single-ion entropies, S_{ion}° , of solids—a route to standard entropy estimation. *Inorg Chem* 48(15):7408–7412. <https://doi.org/10.1021/ic9009543>
- Glasser L, Jenkins HDB (2016) Predictive thermodynamics for ionic solids and liquids. *Physi Chem Chem Phys* 18(31):21226–21240. <https://doi.org/10.1039/C6CP00235H>
- Gotherstrom A, Collins MJ, Angerbjorn A, Liden K (2002) Bone preservation and DNA amplification. *Archaeometry* 44(3):395–404. <https://doi.org/10.1111/1475-4754.00072>
- Gottschall AJ (1958) Heats of formation of hydroxy-, fluor- and chlorapatites. *S Afr J Chem* 11:45–52
- Gramain P, Voegel JC, Gumpfer M, Thomann JM (1987) Surface properties and equilibrium kinetics of hydroxyapatite powder near the solubility equilibrium. *J Colloid Interf Sci* 118(1):148–157. [https://doi.org/10.1016/0021-9797\(87\)90443-7](https://doi.org/10.1016/0021-9797(87)90443-7)
- Grisafe DA, Hummel FA (1970) Pentavalent ion substitutions in the apatite structure part B. *Color J Solid State Chem* 2(2):167–175. [https://doi.org/10.1016/0022-4596\(70\)90065-4](https://doi.org/10.1016/0022-4596(70)90065-4)
- Gu T, Qin S, Wu X (2020) Thermal behavior of pyromorphite ($Pb_{10}(PO_4)_6Cl_2$): In situ high temperature powder X-ray Diffraction Study. *Curr Comput-Aided Drug Des* 10(12):1070. <https://doi.org/10.3390/cryst10121070>
- Harouiya N, Chaïrat C, Köhler SJ, Gout R, Oelkers EH (2007) The dissolution kinetics and apparent solubility of natural apatite in closed reactors at temperatures from 5 to 50 °C and pH from 1 to 6. *Chem Geol* 244(3–4):554–568. <https://doi.org/10.1016/j.chemgeo.2007.07.011>
- Hartnett TQ, Ayyasamy MV, Balachandran PV (2019) Prediction of new iodine-containing apatites using machine learning and density functional theory. *MRS Commun* 9(3):882–890. <https://doi.org/10.1557/mrc.2019.103>
- Hata M, Okada K, Iwai S, Akao M, Aoki H (1978) Cadmium Hydroxyapatite. *Acta Crystall B-Stru* 34(10):3062–3064. <https://doi.org/10.1107/S0567740878010031>
- Hata M, Marumo F, Iwai S, Aoki H (1979) Structure of barium chlorapatite. *Acta Crystall B-Stru* 35(10):2382–2384. <https://doi.org/10.1107/S0567740879009377>
- Hayek E, Petter H (1959) Hydrothermalsynthese von phosphaten zweiwertiger metalle. *Monatsh Chem Verw* 90(4):467–472. <https://doi.org/10.1007/BF00903008>
- Hazen RM (1985) Comparative crystal chemistry and the polyhedral approach. *Rev Mineral* 14:317–346
- Henderson CMB, Bell AMT, Charnock JM, Knight KS, Wendlandt RF, Plant DA, Harrison WJ (2009) Synchrotron X-ray absorption spectroscopy and X-ray powder diffraction studies of the structure of johnbaumite $[Ca_{10}(AsO_4)_6(OH, F)_2]$ and synthetic Pb-, Sr- and Ba-arsenate apatites and some comments on the crystal chemistry of the apatite structure type in general. *Mineral Mag* 73(3):433–455. <https://doi.org/10.1180/minmag.2009.073.3.433>
- Huang YH, Zhu ZQ, Zhang ZL, Zhu YN, Tan LL, Dai LQ, Wei CC (2014) Characterization, dissolution and solubility of mimetite $[Pb_5(AsO_4)_3Cl]$ at 25 °C. In *Appl Mech Mater* 448:15–18. Trans Tech Publications Ltd. <https://doi.org/10.4028/www.scientific.net/AMM.448-453.15>
- Hughes JM, Rakovan JF (2018) The Crystal Structure of Apatite, $Ca_5(PO_4)_3(F, OH, Cl)$. *Rev Mineral Geochem* 48(1):1–12. <https://doi.org/10.2138/rmg.2002.48.1>
- ICDD PDF (1997) International center for diffraction data. Powder Diffraction File, Newtown Square, Pennsylvania, USA
- ICDD (2004) The powder diffraction file, PDF-2
- Inegbenebor AI, Thomas JH, Williams PA (1989) The chemical stability of mimetite and distribution coefficients for pyromorphite-mimetite solid-solutions. *Mineral Mag* 53:363–371. <https://doi.org/10.1180/minmag.1989.053.371.12>
- Islam MI (2021) Solid State Synthesis and Characterization of Apatite Based Ceramic Waste Form for the Immobilization of Radioactive Iodine. Ph. D. thesis, Louisiana State University and Agricultural and Mechanical College
- Ito M, Yamagishi T, Yagasaki H, Kafrawy AH (1995) In vitro properties of a chitosan-bonded bone-filling paste: Studies on solubility of calcium phosphate compounds. *J Biomed Mater Res* 32(1):95–98. [https://doi.org/10.1002/\(SICI\)1097-4636\(199609\)32:1%3c95::AID-JBM11%3e3.0.CO;2-H](https://doi.org/10.1002/(SICI)1097-4636(199609)32:1%3c95::AID-JBM11%3e3.0.CO;2-H)
- Jacques JK (1963) The heats of formation of fluorapatite and hydroxyapatite. *J Chem Sci*. <https://doi.org/10.1039/JR9630003820>
- Jain A, Ong SP, Hautier G, Chen W, Richards WD, Dacek S, Cholia S, Gunter D, Skinner D, Ceder G, Persson KA (2013) Commentary: The Materials Project: A materials genome approach to accelerating materials innovation. *APL Mater* 1(1): 011002. <https://doi.org/10.1063/1.4812323>
- Janicka U, Bajda T, Manecki M (2012) Synthesis and solubility of bromopyromorphite $Pb_5(PO_4)_3Br$. *Mineralogia* 43(1–2):129–135. <https://doi.org/10.2478/v10002-012-0004-4>
- Jaynes WF, Moore Jr PA, Miller DM (1999) Solubility and ion activity products of calcium phosphate minerals (Vol. 28, No. 2, pp.

- 530–536). American Society of Agronomy, Crop Science Society of America, and Soil Science Society of America. <https://doi.org/10.2134/jeq1999.00472425002800020018x>
- Jemal M, Cherifa AB, Khattech I, Ntahomvukiye I (1995) Standard enthalpies of formation and mixing of hydroxy- and fluorapatites. *Thermochim Acta* 259(1):13–21. [https://doi.org/10.1016/0040-6031\(95\)02271-3](https://doi.org/10.1016/0040-6031(95)02271-3)
- Jemal M (2004) Thermochemistry and relative stability of apatite phosphates. *Phosph Res Bull* 15:119–124. https://doi.org/10.3363/prb1992.15.0_119
- Jena H, Venkata Krishnan R, Asuvathraman R, Nagarajan K, Govindan Kutty KV (2011) Thermal expansion and heat capacity measurements on Ba_{10-x}Cs_x(PO₄)₆Cl_{2-δ}, (x=0, 0.5) chloroapatites synthesized by sonochemical process. *J Therm Anal Calorim* 106(3): 875–879. <https://doi.org/10.1007/s10973-011-1715-2>
- Jenkins HDB, Roobottom HK, Passmore J, Glasser L (1999) Relationships among ionic lattice energies, molecular (formula unit) volumes, and thermochemical radii. *Inorg Chem* 38(16):3609–3620. <https://doi.org/10.1021/ic9812961>
- Jenkins DHB, Glasser L (2003) Standard absolute entropy, S°₂₉₈, values from volume or density. 1 inorganic materials. *Inorg Chem* 42:8702–8708. <https://doi.org/10.1021/ic030219p>
- Jenkins HDB, Liebman JF (2005) Volumes of solid state ions and their estimation. *Inorg Chem* 44(18):6359–6372. <https://doi.org/10.1021/ic048341r>
- Johnston CD, Feldmann J, Macphee DE, Worrall F, Skakle JM (2004) Synthesis and proposed crystal structure of a disordered cadmium arsenate apatite Cd₅(AsO₄)₃Cl_{2-δ}, xOH_δ. *Dalton T* 21:3611–3615. <https://doi.org/10.1039/b410483h>
- Junhui Z, Yonghua D, Lishi M, Runyu L (2016) Structural properties, electronic structure and bonding of Ba₁₀(PO₄)₆X₂ (X=F, Cl and Br). *J Alloy Compd* 680:121–128. <https://doi.org/10.1016/j.jallcom.2016.04.114>
- Карбовский В. Л., Сорока А. П., Касияненко В. Х. and Шпак А. П. (2011) Электронно-энергетический ландшафт валентных электронов арсенинатных апатитов кальция и кадмия. Доповіді НАН України. (in Russian)
- Karbovsky VL, Soroka AP (2014) Atomic architecture of vanadate and arsenate calcium and cadmium apatites. *Nanosyst Nanomater Nanotechnol* 12:91–103
- Kelley KK (1960) High-temperature heat-content, heat-capacity, and entropy data for the elements and inorganic compounds. US Bureau of Mines Bull 584:232
- Kelley KK, King EG (1961) Contributions to the data on theoretical metallurgy: XIV. Entropies of the elements and inorganic compounds. In: US Bureau of Mines Bulletin. 592, p. 104. US Government Printing Office, Washington
- Khattech I, Lacout JL, Jemal M (1996) Synthèse et thermochimie des phosphates d'alcalino-terreux. II. Enthalpie standard de formation et de mélange dans les solutions solides d'hydroxyapatites calco-strontiques. In *Annales de chimie* (Paris. 1914) (Vol. 21, No. 4, pp. 259–270)
- Khattech I, Jemal M (1997) Thermochemistry of phosphate products. Part I: Standard enthalpy of formation of tristrontium phosphate and strontium chlorapatite. *Thermochim Acta* 298:17–21. [https://doi.org/10.1016/S0040-6031\(97\)00120-2](https://doi.org/10.1016/S0040-6031(97)00120-2)
- Kim JY, Hunter BA, Fenton RR, Kennedy BJ (1997) Neutron powder diffraction study of lead hydroxyapatite. *Aus J Chem* 50(11):1061–1066. <https://doi.org/10.1071/C97114>
- Kim JY, Fenton RR, Hunter BA, Kennedy BJ (2000) Powder diffraction studies of synthetic calcium and lead apatites. *Aus J Chem* 53(8):679–686. <https://doi.org/10.1071/CH00060>
- Klement R (1936) Basische phosphate zweiwertiger Metalle. I. Basische Magnesiumphosphate. *Z Anorg Allg Chem* 228(3):232–240. <https://doi.org/10.1002/zaac.19362280307>
- Klement R (1939) Basische Phosphate zweiwertiger Metalle. IV. Strontium-Hydroxyapatit. *Z Anorg Allg Chem* 242(2):215–221. <https://doi.org/10.1002/zaac.19392420211>
- Klement R, Zureda F (1940) Basische Phosphate zweiwertiger Metalle V. phosphate und hydroxyapatit des cadmiums. *Z Anorg Allg Chem* 245(3):229–235. <https://doi.org/10.1002/zaac.19402450301>
- Knyazev AV, Bulanov EN, Korokin VZ (2015) Synthesis, structure, and thermal expansion of the Sr₅(AO₄)₃L (A=P, V, Cr; L=F, Cl, Br) apatites. *Inorg Mater* 51(3):245–256. <https://doi.org/10.1134/S0020168515020107>
- Krause J, Bariummanganat V (1955) In Über neue Sauerstoff- und Fluor-haltige Komplexe. VS Verlag für Sozialwissenschaften, Wiesbaden, pp 6–20. https://doi.org/10.1007/978-3-663-04470-3_1
- Kreidler ER, Hummel FA (1970) The crystal chemistry of apatite: structure fields of fluor- and chlorapatite. *Am Mineral J Earth Planet Mater* 55(1–2):170–184
- Krishnan RV, Jena H, Kutty KG, Nagarajan K (2008) Heat capacity of Sr₁₀(PO₄)₆Cl₂ and Ca₁₀(PO₄)₆Cl₂ by DSC. *Thermochim Acta* 478(1–2):13–16. <https://doi.org/10.1016/j.tca.2008.08.009>
- Krivtsov NV, Orlovskii VP, Ezhova ZA, Koval EM (1997) Thermochemistry of hydroxyapatite Ca₁₀(PO₄)₆(OH)₂. *Russ J Inorg Chem* 42(6):791–793
- Kwaśniak-Komitek M, Matusik J, Bajda T, Manecki M, Rakovan J, Marchlewski T, Szala B (2015) Fourier transform infrared spectroscopic study of hydroxylpyromorphite Pb₁₀(PO₄)₆OH₂–hydroxylmimetite Pb₁₀(AsO₄)₆(OH)₂ solid solution series. *Polyhedron* 99:103–111. <https://doi.org/10.1016/j.poly.2015.07.002>
- La Iglesia A, Felix JF (1994) Estimation of thermodynamic properties of mineral carbonates at high and low temperatures from the sum of polyhedral contributions. *Geochim Cosmochim Acta* 58(19):3983–3991. [https://doi.org/10.1016/0016-7037\(94\)90261-5](https://doi.org/10.1016/0016-7037(94)90261-5)
- La Iglesia A (2009) Estimating the thermodynamic properties of phosphate minerals at high and low temperature from the sum of constituent units. *Estud Geol* 65(2):109–119. <https://doi.org/10.3989/egeol.39849.060>
- Latimer WM (1951) Methods of estimating the entropies of solid compounds. *J Am Chem Soc* 73(4):1480–1482
- Latimer WM (1952) Oxidation potentials (Vol. 74, No. 4, p. 333). Prentice-Hall Inc., New York
- Lee YJ, Stephens PW, Tang Y, Li W, Phillips BL, Parise JB, Reeder RJ (2009) Arsenate substitution in hydroxyapatite: structural characterization of the Ca₅(P_xAs_{1-x}O₄)₃OH solid solution. *Am Mineral* 94(5–6):666–675. <https://doi.org/10.1159/000419238>
- LeGeros RZ (1991) Calcium phosphates in oral biology and medicine. *Mon Oral Sci* 15:109–111. <https://doi.org/10.1159/000419238>
- Lei P, Yao T, Gong B, Zhu W, Ran G, Lian J (2020) Spark plasma sintering-densified vanadinite apatite-based chlorine waste forms with high thermal stability and chlorine confinement. *J Nucl Mater* 528:151857. <https://doi.org/10.1016/j.jnucmat.2019.151857>
- Lewis GN, Randall M (1923) Thermodynamics and the free energy of chemical substances. McGraw-Hill, New York
- Li J, Zhu ZQ, Zhu YN, Zhao X, Zhu T (2012) Research progress on solubility of Ca₅(PxAs_{1-x}O₄)₃(OH) and Ca₅(PxAs_{1-x}O₄)₃F. In *Adv Mat Res* (Vol. 518, pp. 888–892). Trans Tech Publications Ltd. <https://doi.org/10.4028/www.scientific.net/AMR.518-523.888>
- Lim SC, Baikie T, Pramana SS, Smith R, White TJ (2011) Apatite metaprism twist angle (φ) as a tool for crystallochemical diagnosis. *J Solid State Chem* 184(11):2978–2986. <https://doi.org/10.1016/j.jssc.2011.08.031>

- Lin J, Zhu Z, Zhu Y, Liu H, Zhang L, Jiang Z (2018) Dissolution and solubility product of Cd-fluorapatite $[Cd_5(PO_4)_3F]$ at pH of 2–9 and 25–45 C. *J Chem.* <https://doi.org/10.1155/2018/3109047>
- Lindsay WL (1979) Chemical equilibria in soils. John Wiley and Sons Ltd., New York
- Lindsay WL, Moreno EC (1960) Phosphate phase equilibria in soils. *Soil Sci Soc Am J* 24(3):177–182. <https://doi.org/10.2136/sssaj1960.03615995002400030016x>
- Liu HL, Zhu YN, Yu HX (2009) Solubility and stability of lead arsenates at 25 C. *J Environ Sci Heal A* 44(13):1465–1475. <https://doi.org/10.1080/10934520903217856>
- Lu F, Yao T, Xu J, Wang J, Scott S, Dong Z, Ewing RC, Lian J (2014) Facile low temperature solid state synthesis of iodoapatite by high-energy ball milling. *RSC Adv* 4(73):38718–38725. <https://doi.org/10.1039/C4RA05320F>
- Mackie PE, Elliot JC, Young RA (1972) Monoclinic structure of synthetic $Ca_5(PO_4)_3Cl$, chlorapatite. *Acta Crystall B-Stru* 28(6):1840–1848. <https://doi.org/10.1107/S0567740872005114>
- Mahapatra PP, Mishra H, Chickerur NS (1982) Solubility and thermodynamic data of cadmium hydroxyapatite in aqueous media. *Thermochim Acta* 54(1–2):1–8. [https://doi.org/10.1016/0040-6031\(82\)85059-4](https://doi.org/10.1016/0040-6031(82)85059-4)
- Mahapatra PP, Mahapatra LM, Mishra B (1987) Arsenate hydroxyapatite: A physico-chemical and thermodynamic investigation. *Polyhedron* 6(5):1049–1052. [https://doi.org/10.1016/S0277-5387\(00\)80953-5](https://doi.org/10.1016/S0277-5387(00)80953-5)
- Mahapatra PP, Mahapatra LM, Mishra B (1989) Physicochemical studies on solid solutions of calcium phosphorus arsenic hydroxyapatites. *Bull Chem Soc Jpn* 62(10):3272–3277. <https://doi.org/10.1246/bcsj.62.3272>
- Manca SG, Botto IL, Baran EJ (1980) Die IR-Spektren einiger Arsenat-Halogen-Apatite. *Monatsh Chem.* 111(4): 949–955. <https://doi.org/10.1007/BF00899261>
- Manecki M, Maurice PA (2008) Siderophore promoted dissolution of pyromorphite. *Soil Sci* 173(12):821–830. <https://doi.org/10.1097/SS.0b013e31818e8968>
- Manecki M, Maurice PA, Traina SJ (2000) Uptake of aqueous Pb by Cl⁻, F⁻, and OH⁻ apatites: mineralogic evidence for nucleation mechanisms. *Am Mineral* 85(7–8):932–942. <https://doi.org/10.2138/am-2000-0707>
- Marchenko VI, Getman EI, Parikina AV (2003) Solid-state synthesis of $Sr_5(VO_4)_3OH$ and its interaction with $Ca_5(VO_4)_3OH$. *Украинский Химический Журнал* 69(11–12):70–74
- Marcus Y (1987) The thermodynamics of solvation of ions. Part 2.—The enthalpy of hydration at 298.15 K. *J Chem Soc Farad T 83(2):339–349.* <https://doi.org/10.1039/F19878300339>
- Mathew M, Mayer I, Dickens B, Schroeder LW (1979) Substitution in barium-fluoride apatite: the crystal structures of $Ba_{10}(PO_4)_6F_2$, $Ba_6La_2Na_2(PO_4)_6F_2$ and $Ba_4Nd_2Na_3(PO_4)_6F_2$. *J Solid State Chem* 28(1):79–95. [https://doi.org/10.1016/0022-4596\(79\)90061-6](https://doi.org/10.1016/0022-4596(79)90061-6)
- Mayer I, Wahnon S, Cohen S (1979) Preparation of hydroxyapatites via the MSO4 sulphates (M= Ca, Sr, Pb and Eu). *Mater Res Bull* 11:1479–1483. [https://doi.org/10.1016/0025-5408\(79\)90092-8](https://doi.org/10.1016/0025-5408(79)90092-8)
- McCann HG (1968) The solubility of fluorapatite and its relationship to that of calcium fluoride. *Arch Oral Biol* 13(8):987–1001. [https://doi.org/10.1016/0003-9969\(68\)90014-9](https://doi.org/10.1016/0003-9969(68)90014-9)
- McConnell D (1974) The crystal chemistry of apatite. *B Mineral* 97(2):237–240
- McDowell H, Gregory TM, Brown WE (1977) Solubility of $Ca_5(PO_4)_3OH$ in the system $Ca(OH)_2$ – H_3PO_4 – H_2O at 5, 15, 25, and 37 C. *J Res NBS a* 81:273–281. <https://doi.org/10.6028/jres.081A.017>
- Mercier PH, Dong Z, Baikie T, Le Page Y, White TJ, Whitfield PS, Mitchel LD (2007) Ab initio constrained crystal-chemical Rietveld refinement of $Ca_{10}(VxP1-xO_4)6F_2$ apatites. *Acta Crystallogr Section b* 63(1):37–48. <https://doi.org/10.1107/S0108768106045538>
- Merker L, Wondratschek H (1957) Neue Verbindungen mit apatitartiger Struktur II. Die Gruppe der Alkali-Blei-Verbindungen. *Z. Krist-Cryst. Mater.* 109(1–6): 110–114. <https://doi.org/10.1524/zkri.1957.109.16.110>
- Merker L, Wondratschek H (1959) Bleiverbindungen mit Apatitstruktur, insbesondere Blei-Jod-und Blei-Brom-Apatite. *Z Anorg All Chem* 300(1–2):41–50. <https://doi.org/10.1002/zaac.1959300104>
- Mooney RW, Aia MA (1961) Alkaline Earth Phosphates. *Chem Rev* 61(5):433–462
- Moreno EC, Gregory TM, Brown WE (1968) Preparation and solubility of hydroxyapatite. *J Res NBS a Phys Ch* 72(6):773. <https://doi.org/10.6028/jres.072A.052>
- Moreno EC, Aoba T (1991) Comparative solubility study of human dental enamel, dentin, and hydroxyapatite. *Calcified Tissue Int* 49(1):6–13. <https://doi.org/10.1007/BF02555895>
- Mungmode CD, Gahane DH, Moharil SV (2018) Wet chemical synthesis and luminescence in $Ca_5(PO_4)_3M$: Eu²⁺ (M= Br, I) phosphors for solid state lighting. In AIP Conference Proceedings (Vol. 1953, No. 1, p. 060037). AIP Publishing LLC. <https://doi.org/10.1063/1.5032768>
- Nakamura M, Oqmhula K, Utimula K, Eguchi M, Oka K, Hongo K, Maeda K (2020) Light absorption properties and electronic band structures of lead-vanadium oxyhalide apatites $Pb_5(VO_4)_3X$ (X= F, Cl, Br, I). *Chem Asian J* 15(4): 540–545. <https://doi.org/10.1002/asia.201901692>
- Narasaraju TSB, Rao KK, Rai US (1979) Determination of solubility products of hydroxylapatite, chlorapatite, and their solid solutions. *Can J Chem* 57(15):1919–1922. <https://doi.org/10.1139/v79-307>
- Newberry NG, Essene EJ, Peacor DR (1981) Alforsite, a new member of the apatite group: the barium analogue of chlorapatite. *Am Mineral* 66(9–10):1050–1053
- Noel MC (2018) Aqueous precipitation of crystalline svabite ($Ca_5(AsO_4)_3F$) and svabite/fluorapatite ($Ca_5(AsO_4)_X(PO_4)_{3-X}F$) compounds and evaluation of their stability. Ph. D. thesis, McGill University
- Nötzold D, Wulff H, Herzog G (1994) Differenzthermoanalyse der Bildung des Pentastrontiumchloridphosphats und röntgenographische Untersuchungen seiner Struktur. *J Alloys Compd* 215:281–288. [https://doi.org/10.1016/0925-8388\(94\)90855-9](https://doi.org/10.1016/0925-8388(94)90855-9)
- Nriagu JO (1973) Lead orthophosphates—II. Stability of chalopyromophite at 25 C. *Geochim. et Cosmochim. Ac.* 37(3): 367–377. [https://doi.org/10.1016/0016-7037\(73\)90206-8](https://doi.org/10.1016/0016-7037(73)90206-8)
- Ntahomvukiye I, Khattech I, Jemal M (1997) Synthèse, caractérisation et thermochimie d'apatites calco-plombeuses fluorées $Ca_{(10-x)}Pb_x(PO_4)_6F_2$, $0 \leq x \leq 10$. *Annales De Chimie Science Des Matériaux* 22:435–446 ((in French))
- O'Donnell MD, Hill RG, Fong SK (2009) Neutron diffraction of chlorine substituted fluorapatite. *Mater Lett* 63(15):1347–1349. <https://doi.org/10.1016/j.matlet.2009.03.020>
- Oelkers EH, Montel JM (2008) Phosphates and nuclear waste storage. *Elements* 4(2):113–116. <https://doi.org/10.2113/GSELEMENTS.4.2.113>
- Oelkers EH, Valsami-Jones E (2008) Phosphate mineral reactivity and global sustainability. *Elements* 4(2):83–87. <https://doi.org/10.2113/GSELEMENTS.4.2.83>
- Oelkers EH, Schott J (Eds.). (2018) Thermodynamics and kinetics of water-rock interaction (Vol. 70). Walter de Gruyter GmbH & Co KG
- Oka K, Takasu M, Nishiki W, Nishikubo T, Azuma M, Noma N, Iwasaki M (2022) Negative thermal expansion in fluoroapatite $Pb_5(VO_4)_3F$ enhanced by the steric effect of Pb²⁺. *Inorg Chem*

- 61(32):12552–12558. <https://doi.org/10.1021/acs.inorgchem.2c01300>
- Okudera H (2013) Relationships among channel topology and atomic displacements in the structures of $\text{Pb}_5(\text{BO}_4)_3\text{Cl}$ with B=P (pyromorphite), V (vanadinite), and As (mimetite). *Am Mineral* 98(8–9):1573–1579. <https://doi.org/10.2138/am.2013.4417>
- Olds TA, Kampf AR, Rakovan JF, Burns PC, Mills OP, Laughlin-Yurs C (2021) Hydroxylpyromorphite, a mineral important to lead remediation: Modern description and characterization. *Am Mineral* 106(6):922–929. <https://doi.org/10.2138/am-2021-7516>
- Pan Y, Fleet ME (2002) Compositions of the apatite-group minerals: substitution mechanisms and controlling factors. *Rev Mineral Geochem* 48(2):13–49. <https://doi.org/10.2138/rmg.2002.48.2>
- Pasero M, Kampf AR, Ferraris C, Pekov IV, Rakovan J, White TJ (2010) Nomenclature of the apatite supergroup minerals. *Eur J Mineral* 22(2):163–179. <https://doi.org/10.1127/0935-1221/2010/0022-2022>
- Pekov IV, Koshlyakova NN, Zubkova NV, Krzatała A, Galuskina IO, Belakovskiy DI, Galuskin EV, Britvin SN, Sidorov EG, Vapnik Y, Pushcharovsky DY (2021) Pliniusite, $\text{Ca}_5(\text{VO}_4)_3\text{F}$, a new apatite-group mineral and the novel natural ternary solid-solution system pliniusite–svabite–fluorapatite. *Am Mineral* (in Press). <https://doi.org/10.2138/am-2022-8100>
- Phebe DE, Narasaraju TSB (1995) Preparation and characterization of hydroxyl and iodide apatites of calcium and their solid solutions. *J Mater Sci Lett* 14(4):229–231. <https://doi.org/10.1007/BF00275606>
- Pieczka A, Biagioni C, Gołębiewska B, Jeleń P, Pasero M, Sitarz M (2018) Parafiniukite, $\text{Ca}_2\text{Mn}_3(\text{PO}_4)_3\text{Cl}$, a new member of the apatite supergroup from the Szklary pegmatite, Lower Silesia, Poland: description and crystal structure. *Minerals* 8(11):485. <https://doi.org/10.3390/min8110485>
- Posner AS, Perloff A, Diorio AF (1958) Refinement of the hydroxyapatite structure. *Acta Crystallogr* 11(4):308–309. <https://doi.org/10.1107/S0365110X58000815>
- Ptáček P (2016) Synthetic phase with the structure of apatite. In Chemistry: Apatites and their synthetic analogues—synthesis, structure, properties and applications (pp. 177–244). INTECH
- Puzio B, Manecki M, Kwaśniaki-Kominek M (2018) Transition from endothermic to exothermic dissolution of hydroxyapatite $\text{Ca}_5(\text{PO}_4)_3\text{OH}$ –johnbaumite $\text{Ca}_5(\text{AsO}_4)_3\text{OH}$ solid solution series at temperatures ranging from 5 to 65°C. *Minerals* 8:281. <https://doi.org/10.3390/min8070281>
- Puzio B, Solecka U, Topolska J, Manecki M, Bajda T (2021) Solubility and dissolution mechanisms of vanadinite $\text{Pb}_5(\text{VO}_4)_3\text{Cl}$: effects of temperature and PO_4 substitutions. *Appl Geochem* 131:105015. <https://doi.org/10.1016/j.apgeochem.2021.105015>
- Puzio B, Zhang L, Szymanowski JES, Burns PC, Manecki M (2022) Thermodynamic characterization of synthetic lead–arsenate apatites with different halogen substitutions. *Am Mineral*. <https://doi.org/10.2138/am-2020-7452>
- Rakovan JF, Hughes JM (2000) Strontium in the apatite structure: strontian fluorapatite and belovite-(Ce). *Can Mineral* 38(4):839–845. <https://doi.org/10.2113/gscammin.38.4.839>
- Rakovan JF, Pasteris JD (2015) A technological gem: Materials, medical, and environmental mineralogy of apatite. *Elements* 11(3):195–200. <https://doi.org/10.2113/gselements.11.3.195>
- Rakovan J, Scovil JA (2021) Apatite and the apatite supergroup. *Rocks Miner* 96(1):13–19. <https://doi.org/10.1080/00357529.2021.1827906>
- Robie RA, Hemingway BS, Fischer JR (1979) Thermodynamic Properties of Minerals and Related Substances at 298.15 K and 1 Bar (105 Pascals) Pressure and at Higher Temperatures. *Geol Survey Bull* 1452: 456
- Robie RA, Hemingway BS (1995) Thermodynamic properties of minerals and related substances at 298.15 K and 1 bar (105 Pascals) pressure and at higher temperatures, 2131, 461 p. US Government Printing Office, Washington
- Roh YH, Hong ST (2005) Apatite-type $\text{Ba}_5(\text{VO}_4)_3\text{Cl}$. *Acta Crystallogr E* 61(8):i140–i142. <https://doi.org/10.1107/S1600536805018854>
- Roine A (1994) Outokumpu HSC chemistry for windows. Chemical Reaction and Equilibrium Software with Extensive Thermochemical Database
- Rollin-Martinet S, Navrotsky A, Champion E, Grossin D, Drouet C (2013) Thermodynamic basis for evolution of apatite in calcified tissues. *Am Mineral* 98:2037–2045. <https://doi.org/10.2138/am-2013.4537>
- Rossini FD, Gucker FT Jr, Johnston HL, Pauling L, Vinal GW (1952) Status of the values of the fundamental constants for physical chemistry as of July 1, 1951 I. *J Am Chem Soc* 74(11):2699–2701
- Santillan-Medrano J, Jurinak JJ (1975) The chemistry of lead and cadmium in soil: solid phase formation. *Soil Sci Soc Am J* 39(5):851–856. <https://doi.org/10.2136/sssaj1975.03615995003900050020x>
- Sassani DC, Shock EL (1992) Estimation of standard partial molal entropies of aqueous ions at 25°C and 1 bar. *Geochim Cosmochim Acta* 56(11):3895–3908. [https://doi.org/10.1016/0016-7037\(92\)90004-3](https://doi.org/10.1016/0016-7037(92)90004-3)
- Shellis RP, Wahab FK, Heywood BR (1993) The hydroxyapatite ion activity product in acid solutions equilibrated with human enamel at 37°C. *Caries Res* 27(5):365–372. <https://doi.org/10.1159/000261566>
- Shock EL, Sassani DC, Willis M, Sverjensky DA (1997) Inorganic species in geologic fluids: correlations among standard molal thermodynamic properties of aqueous ions and hydroxide complexes. *Geochim Cosmochim Acta* 61(5):907–950. [https://doi.org/10.1016/S0016-7037\(96\)00339-0](https://doi.org/10.1016/S0016-7037(96)00339-0)
- Smirnova ZG, Illarionov VV, Volkovich SI (1962) Heats of formation of fluorapatite and hydroxyl apatite and the α and β modifications of tricalcium phosphate. *Zhur Neorg Khim* 7:1779–1782
- Solecka U, Bajda T, Topolska J, Zelek-Pogudz S, Manecki M (2018) Raman and Fourier transform infrared spectroscopic study of pyromorphite–vanadinite solid solutions. *Spectrochim Acta A* 190:96–103. <https://doi.org/10.1016/j.saa.2017.08.061>
- Sordyl J, Puzio B, Manecki M, Borkiewicz O, Topolska J, Zelek-Pogudz S (2020) Structural assessment of fluorine, chlorine, bromine, iodine, and hydroxide substitutions in lead arsenate apatites (Mimetites)– $\text{Pb}_5(\text{AsO}_4)_3\text{X}$. *Minerals* 10(6):494. <https://doi.org/10.3390/min10060494>
- Stefánsson A (2001) Dissolution of primary minerals of basalt in natural waters: I. Calculation of mineral solubilities from 0°C to 350°C. *Chem Geol* 172(3–4):225–250. [https://doi.org/10.1016/S0009-2541\(00\)00263-1](https://doi.org/10.1016/S0009-2541(00)00263-1)
- Stennett MC, Pinnock IJ, Hyatt NC (2011) Rapid synthesis of $\text{Pb}_5(\text{VO}_4)_3\text{I}$, for the immobilisation of iodine radioisotopes, by microwave dielectric heating. *J Nucl Mater* 414(3):352–359. <https://doi.org/10.1016/j.jnucmat.2011.04.041>
- Stumm W, Morgan JJ (2012) Aquatic chemistry: chemical equilibria and rates in natural waters. John Wiley & Sons, New York
- Sudarsanan KT, Young RA (1969) Significant precision in crystal structural details Holly Springs Hydroxyapatite. *Acta Crystall B-Stru* 25(8):1534–1543. <https://doi.org/10.1107/S0567740869004298>
- Sudarsanan K, Mackie PE, Young RA (1972) Comparison of synthetic and mineral fluorapatite, $\text{Ca}_5(\text{PO}_4)_3\text{F}$, in crystallographic detail. *Mater Res Bull* 7(11):1331–1337. [https://doi.org/10.1016/0025-5408\(72\)90113-4](https://doi.org/10.1016/0025-5408(72)90113-4)
- Sudarsanan K, Young RA (1974) Structure refinement and random error analysis for strontiumchlorapatite, $\text{Sr}_5(\text{PO}_4)_3\text{Cl}$. *Acta*

- Crystall B-Stru 30(6):1381–1386. <https://doi.org/10.1107/S056740874004936>
- Sudarsanan K, Young RA, Wilson AJC (1977) The structures of some cadmiumapatites Cd₅(MO₄)₃X. I. determination of the structures of Cd₅(VO₄)₃I, Cd₅(PO₄)₃Br, Cd₃(AsO₄)₃Br and Cd₅(VO₄)₃Br. Acta Crystall B Stru 33(10):3136–3142. <https://doi.org/10.1107/S0567740877010413>
- Sudarsanan K, Young RA (1978) Structural interactions of F, Cl and OH in apatites. Acta Crystall B-Stru 34(5):1401–1407. <https://doi.org/10.1107/S0567740878005798>
- Suetsugu Y (2014) Synthesis of lead vanadate iodoapatite utilizing dry mechanochemical process. J Nucl Mater 454(1–3):223–229. <https://doi.org/10.1016/j.jnucmat.2014.07.073>
- Sverjensky DA, Shock EL, Helgeson HC (1997) Prediction of the thermodynamic properties of aqueous metal complexes to 1000 °C and 5 kb. Geochim Cosmochim Acta 61(7):1359–1412. [https://doi.org/10.1016/S0016-7037\(97\)00009-4](https://doi.org/10.1016/S0016-7037(97)00009-4)
- Swafford SH, Holt EM (2002) New synthetic approaches to monophosphate fluoride ceramics: synthesis and structural characterization of Na₂Mg(PO₄)F and Sr₅(PO₄)₃F. Solid State Sci 4(6):807–812. [https://doi.org/10.1016/S1293-2558\(02\)01297-9](https://doi.org/10.1016/S1293-2558(02)01297-9)
- Tacker RC, Stormer JC (1989) A thermodynamic model for apatite solid solutions, applicable to high-temperature geologic problems. Am Mineral 74:877–888
- Tait K, Ball NA, Hawthorne FC (2015) Pieczkaite, ideally Mn₅(PO₄)₃Cl, a new apatite-supergroup mineral from Cross Lake, Manitoba, Canada: Description and crystal structure. Am Mineral 100(5–6):1047–1052. <https://doi.org/10.2138/am-2015-5117>
- Tardy Y, Vieillard P (1977) Relationships among Gibbs free energies and enthalpies of formation of phosphates, oxides and aqueous ions. Contrib Mineral Petr 63(1):75–88. <https://doi.org/10.1007/BF00371677>
- Topolska J, Manecki M, Bajda T, Borkiewicz O, Budzewski P (2016) Solubility of pyromorphite Pb₅(PO₄)₃Cl at 5–65 °C and its experimentally determined thermodynamic parameters. J Chem Therm 98:282–287. <https://doi.org/10.1016/j.jct.2016.03.031>
- Topolska J, Puzio B, Borkiewicz O, Sordyl J, Manecki M (2021) Solubility product of vanadinite Pb₅(VO₄)₃Cl at 25 °C—a comprehensive approach to incongruent dissolution modeling. Minerals 11(2):135. <https://doi.org/10.3390/min11020135>
- Trotter J, Barnes WH (1958) The structure of vanadinite. Canad Mineral 6(2):161–173
- Valsami-Jones E, Ragnarsdottir KV, Putnis A, Bosbach D, Kemp AJ, Cressey G (1998) The dissolution of apatite in the presence of aqueous metal cations at pH 2–7. Chem Geol 151(1–4):215–233. [https://doi.org/10.1016/S0009-2541\(98\)00081-3](https://doi.org/10.1016/S0009-2541(98)00081-3)
- Valyashko VM, Kogarko LN, Khodakovskiy IL (1968) Stability of fluorapatite, chlorapatite, and hydroxyapatite in aqueous solutions at different temperatures. Geochem Int 5:21–30
- Verbeeck RM, Hauben M, Thun HP, Verbeek F (1977) Solubility and solution behaviour of strontiumhydroxyapatite. Z Phys Chem 108(2):203–215. <https://doi.org/10.1524/zpch.1977.108.2.203>
- Vieillard P, Tardy Y (1984) Thermochemical properties of phosphates. In: Nriagu JO, Moore PB (eds) Phosphate Minerals. Springer, Berlin, pp 171–198
- Vieillard P (2000) A new method for the prediction of Gibbs free energies of formation of hydrated clay minerals based on the electronegativity scale. Clay Clay Miner 48(4):459–473. <https://doi.org/10.1346/CCMN.2000.0480406>
- Vieillard P, Tardy Y (1988) Estimation of enthalpies of formation of minerals based on their refined crystal structures. Am J Sci 288(10):997–1040. <https://doi.org/10.2475/ajs.288.10.997>
- Wagman DD, Evans WH, Parker VB, Schumm RH, Halow I, Bailey SM, Churney KL, Nuttall RL (1982) The NBS tables of chemical thermodynamic properties. Selected values for inorganic and C1 and C2 organic substances in SI units. National Standard Reference Data System, New York
- Wang J (2015) Incorporation of iodine into apatite structure: a crystal chemistry approach using Artificial Neural Network. Front Earth Sci 3:20. <https://doi.org/10.3389/feart.2015.00020>
- Wardojo TA, Hwu SJ (1996) Chlorapatite: Ca₅(AsO₄)₃Cl. Acta Crystall c 52:2959–2960. <https://doi.org/10.1107/S0108270196011006>
- Weil M, Đorđević T, Lengauer CL, Kolitsch U (2009) Investigations in the systems Sr–As–O–X (X=H, Cl): Preparation and crystal structure refinements of the anhydrous arsenates (V) Sr₃(AsO₄)₂, Sr₂As₂O₇, α-and β-SrAs₂O₆, and of the apatite-type phases Sr₅(AsO₄)₃OH and Sr₅(AsO₄)₃Cl. Solid State Sci 11(12):2111–2117. <https://doi.org/10.1016/j.solidstatosciences.2009.08.019>
- White TJ, Dong Z (2003) Structural derivation and crystal chemistry of apatites. Acta Crystall B-Stru 59(1):10–16. <https://doi.org/10.1107/S0108768102019894>
- Witkowska M, Motyka J, Kwaśniak-Kominek M, Manecki M (2014) Halogen substitution in synthetic lead apatite compounds Raman spectroscopy study. Geol Geophys Environ 40(1):141–142
- Wołowiec M, Tuchowska M, Kudła P, Bajda T (2019) Synthesis and characterization of cadmium chlorapatite Cd 5(PO₄)₃Cl. Mineralogia 50(1–4):3–12
- Xie L, Giammar DE (2007) Equilibrium solubility and dissolution rate of the lead phosphate chloropyromorphite. Environ Sci Technol 41(23):8050–8055. <https://doi.org/10.1021/es071517e>
- Yan Q, Zhu Y, Feng G, Zhu Z, Zhang L, Liu J, He H (2020) Characterization, dissolution and solubility of lead fluorapatite at 25–45 °C. Appl Geochem 120:104659–104668. <https://doi.org/10.1016/j.apgeochem.2020.104659>
- Yoder CH, Flora NJ (2005) Geochemical applications of the simple salt approximation to the lattice energies of complex materials. Am Mineral 90(2–3):488–496. <https://doi.org/10.2138/am.2005.1537>
- Yoder CH, Rowand JP (2006) Application of the simple salt lattice energy approximation to the solubility of minerals. Am Mineral 91(5–6):747–752. <https://doi.org/10.2138/am.2006.2073>
- Yuan Z, Gao T, Zheng Y, Ma S, Yang M, Chen P (2017) First-principles study on structural, electronic, vibrational and thermodynamic properties of Sr₁₀(PO₄)₆X₂ (X= F, Cl, Br). RSC Adv 7(48):30310–30319. <https://doi.org/10.1039/C7RA04359G>
- Zhang X, Zhu Y, Zeng H, Wang D, Liu J, Liu H, Xu L (2011) Dissolution and solubility of the arsenate–phosphate hydroxylapatite solid solution [Ca₅(P_xAs_{1-x}O₄)₃(OH)] at 25 °C. Environ Chem 8(2):133–145. <https://doi.org/10.1071/EN10102>
- Zhang F, Zhang F, Jing Q, Pan S, Yang Z, Jia D (2015) Synthesis, crystal structure and properties of the strontium vanadate fluoride Sr₅(VO₄)₃F. Z Anorg Allg Chem 641(7):1211–1215. <https://doi.org/10.1002/zaac.201500079>
- Zheng Y, Gao T, Gong Y, Ma S, Yang M, Chen P (2015) Electronic, vibrational and thermodynamic properties of Ca₁₀(AsO₄)₆(OH)₂: first principles study. Eur Phys J Appl Phys. <https://doi.org/10.1051/epjp/2015150301>
- Zhu C, Sverjensky DA (1991) Partitioning of F-Cl-OH between minerals and hydrothermal fluids. Geochim Cosmochim Ac 55:1837–1858. [https://doi.org/10.1016/0016-7037\(91\)90028-4](https://doi.org/10.1016/0016-7037(91)90028-4)
- Zhu YN, Zhang XH, Xie QL, Wang DQ, Cheng GW (2006) Solubility and stability of calcium arsenates at 25 °C. Water Air Soil Poll 169(1):221–238. <https://doi.org/10.1007/s11270-006-2099-y>
- Zhu Y, Zhang X, Chen Y, Xie Q, Lan J, Qian M, He N (2009) A comparative study on the dissolution and solubility of hydroxylapatite and fluorapatite at 25 °C and 45 °C. Chem Geol 268(1–2):89–96. <https://doi.org/10.1016/j.chemgeo.2009.07.014>
- Zhu Y, Zhang X, Zeng H, Liu H, He N, Qian M (2011) Characterization, dissolution and solubility of synthetic svabite [Ca₅(AsO₄)₃F] at 25–45 °C. Environ Chem Lett 9:339–345. <https://doi.org/10.1007/s10311-010-0284-0>

Zhu Y, Zhu Z, Zhao X, Liang Y, Huang Y (2015a) Characterization, dissolution, and solubility of lead hydroxypyromorphite [$\text{Pb}_5(\text{PO}_4)_3\text{OH}$] at 25–45 °C. J Chem-NY. <https://doi.org/10.1155/2015/269387>

Zhu Y, Zhu Z, Zhao X, Liang Y, Dai L, Huang Y (2015b) Characterization, dissolution and solubility of synthetic cadmium hydroxylapatite [$\text{Cd}_5(\text{PO}_4)_3\text{OH}$] at 25–45° C. Geochem Trans 16(1):1–11. <https://doi.org/10.1186/s12932-015-0025-1>

Zhu Y, Huang B, Zhu Z, Liu H, Huang Y, Zhao X, Liang M (2016) Characterization, dissolution and solubility of

the hydroxypyromorphite–hydroxyapatite solid solution [$(\text{Pb}_x\text{Ca}_{1-x})_5(\text{PO}_4)_3\text{OH}$] at 25 °C and pH 2–9. Geochem Trans 17(1):1–18. <https://doi.org/10.1186/s12932-016-0034-8>

Publisher's Note Springer Nature remains neutral with regard to jurisdictional claims in published maps and institutional affiliations.